



Die Grenzen der
Chemie neu ausloten?
It takes
#HumanChemistry

Wir suchen kreative Chemikerinnen und Chemiker,
die mit uns gemeinsam neue Wege gehen wollen –
mit Fachwissen, Unternehmertum und Kreativität für
innovative Lösungen. Informieren Sie sich unter:

evonik.de/karriere

Novel Bilayer Microarray Patch-Assisted Long-Acting Micro-Depot Cabotegravir Intradermal Delivery for HIV Pre-Exposure Prophylaxis

Ismail A. Tekko, Lalitkumar K. Vora, Fabiana Volpe-Zanutto, Kurtis Moffatt, Courtney Jarrahan, Helen O. McCarthy, and Ryan F. Donnelly*

Injectable long-acting cabotegravir (CAB LA) is effective and safe for pre-exposure HIV prophylaxis. It is recently approved for clinical use in those at high risk of contracting HIV. However, injections are invasive and access to trained healthcare personnel to administer CAB LA can be limited, especially in low-income countries (LICs). Herein, for the first time, the development of a bilayer microarray patch (MAP) with unique design and novel formulation as a potential alternative self-administrated intradermal delivery system for CAB is reported. The novel MAP has a high drug load (≈ 3 mg/0.5 cm² of CAB LA or its micronized sodium salt) and fast-dissolving tips (<30 min) and shows good mechanical properties and skin insertion capabilities. Importantly, in preclinical in vivo studies using Sprague Dawley rats, this MAP is able to implant the drug-loaded tips in the skin, forming micro-depots. Both drug forms are then released in a sustained manner, maintaining human therapeutic levels in the rats for one month after a single application. Weekly repeated MAP dosing in the rats showed the MAPs to be reproducible and well-tolerated. This bilayer MAP presents a promising minimally-invasive, self-administered, alternative delivery system for CAB for enhanced HIV prevention, especially in LICs.

1. Introduction

Human immunodeficiency virus (HIV) remains a global epidemic.^[1] More than 76 million people have been infected and 33 million people have died of HIV/AIDS since the beginning of the epidemic. Globally, 38.0 million people were living with HIV at the end of 2019.^[2] More than 25.7 million of the infected people, which represents $\approx 67.8\%$ of the global HIV cases, are located in low-income countries (LICs), mostly in sub-Saharan Africa.^[3]

Several strategies have been introduced to prevent HIV infection, including i) using condoms, ii) limiting the number of sexual partners, iii) abstinence (not having sex), and iv) avoiding reuse or sharing of hypodermic needles, all with limited success.^[4] Antiretroviral (ARV) drugs emerged in the mid-1990s, revolutionizing the treatment of HIV-1 (the most common pathogenic strain of the virus) infection and reducing the previously high rate of HIV infections.^[5] Since then, many ARV drugs have


been developed. They are currently classified into five categories; nucleoside reverse transcriptase inhibitors, non-nucleoside reverse transcriptase inhibitors, protease inhibitors, entry inhibitors, and integrase inhibitors.^[1] These drugs are used for treatment, and some are also licensed for use for prevention either as a pre-exposure (also called pre-exposure prophylaxis (PrEP)) or post-exposure (called post-exposure prophylaxis (PEP)) measure. While PrEP is defined as administering an ARV drug to HIV-negative individuals at high risk of infection, PEP is defined as administering an ARV drug to HIV-negative individuals after a potential exposure (occupational or sexual), ideally within 72 h. Both treatment and prevention have been shown to be effective in reducing the rate of HIV infection.^[6] However, the high cost per HIV patient for lifetime treatment with multiple ARVs makes PrEP an attractive and cost-effective approach.^[7] Despite the success of widespread ARV use, new HIV infections continue to emerge. In 2018, an estimated 1.7 million new infections occurred.^[8] One of the main issues that reduce the effective use of the ARV therapy is patient compliance/adherence.^[9]

Cabotegravir (CAB) is an integrase strand transfer inhibitor developed by ViiV Healthcare for treatment in combination

I. A. Tekko, L. K. Vora, F. Volpe-Zanutto, K. Moffatt, H. O. McCarthy, R. F. Donnelly
School of Pharmacy
Medical Biology Centre
Queen's University Belfast
97 Lisburn Road, Belfast, Northern Ireland BT97BL, UK
E-mail: R.Donnelly@qub.ac.uk

I. A. Tekko
Faculty of Pharmacy
Aleppo University
Aleppo, Syria

C. Jarrahan
PATH
2201 Westlake Avenue, Seattle, WA 98121, USA

 The ORCID identification number(s) for the author(s) of this article can be found under <https://doi.org/10.1002/adfm.202106999>.

© 2021 The Authors. Advanced Functional Materials published by Wiley-VCH GmbH. This is an open access article under the terms of the Creative Commons Attribution License, which permits use, distribution and reproduction in any medium, provided the original work is properly cited.

DOI: 10.1002/adfm.202106999

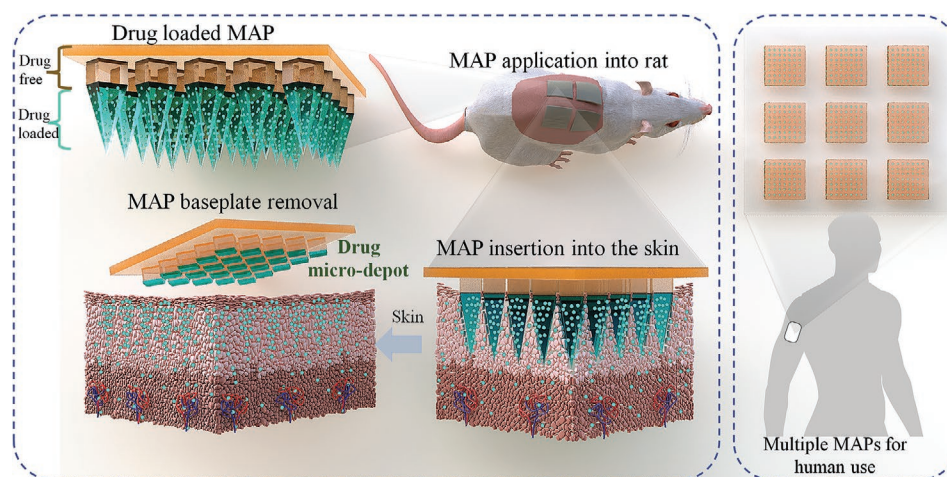


Figure 1. Schematic depiction of programmed-dissolving bilayer MAP with high drug loading for efficient ID long-acting micro-depot drug delivery for HIV PrEP for potential monthly/weekly application in humans.

with rilpivirine or used alone for PrEP, of HIV-1 infections.^[10,11] CAB is a highly hydrophobic drug produced in micronized forms, either as a free acid (CAB FA) or sodium salt (CAB Na). The water-solubilities of CAB FA and CAB Na are ≈ 0.113 and 0.446 mg mL^{-1} , respectively.^[12]

ViiV Healthcare has also developed CAB LA for intramuscular (IM) injection from its micronized form (CAB FA). The innovative CAB LA formulation is highly effective, safe, and well-tolerated in animals and humans, and it exhibits an increased half-life of ≈ 40 days (25–52 days).^[13] This drug has recently been approved for monthly (400 mg) administration for HIV treatment (in combination with IM rilpivirine LA as CABENUVA), following a 30-day lead-in period of 30 mg CAB Na oral tablets and a loading dose injection of 800 mg of CAB LA.^[14] Furthermore, a supplemental New Drug Application has been submitted to the US Food and Drug Administration (US FDA) to expand the labeling indication for CABENUVA for delivery every two months, based on the results of the ATLAS-2M clinical trial.^[15] Now, phase 3 clinical trials have also been completed, showing that bimonthly injection of 600 mg of CAB LA is 89% more effective than daily oral tenofovir/emtricitabine for PrEP in women and is also superior in preventing HIV infection in men who have sex with men and transgender women.^[16] Nevertheless, in addition to being relatively expensive to manufacture, CAB LA IM injection is painful,^[17] and requires trained health care professionals for administration, which again may affect patient compliance and adherence to therapy, especially in the endemic regions of LICs, where access to trained health care professionals is limited. Furthermore, misuse and inappropriate disposal of needles are also problems of particular significance in LICs, potentially leading to the transmission of blood-borne diseases. Indeed, recent studies carried out over 6–12 month periods assessing the frequency of needle-stick injuries in clinical settings have shown the prevalence of such injuries in health care workers to be high over the specific reporting periods of the studies: 51% in Benin City, Nigeria;^[18] 52.7% in Asaba city, Nigeria; 83.8% in Minna, Nigeria;^[19] and 86.1% in New Delhi, India.^[20] Therefore,

an alternative drug delivery system that addresses these limitations is highly desirable.

Dissolving microarray patch (MAP), also known as microneedle arrays, is an innovative alternative drug delivery system which has been used successfully to deliver a wide range of drug molecules and vaccines intra- and trans-dermally.^[21,22] MAP contains micron-scale projections often made from self-dissolving biocompatible water-soluble polymers that can painlessly, and without drawing blood, penetrate the outermost layer of the skin, the stratum corneum. Upon MAP application, such projections dissolve quickly, depositing their drug payload in the viable skin layers for subsequent absorption by the rich dermal microcirculation.^[22,23] A dissolving MAP can potentially be self-administered, reducing the burden on health care workers after a patient has learned to administer the dose.^[24,25] Although dissolving MAPs have been used successfully to deliver a wide range of drug molecules, including hydrophilic and hydrophobic drugs and vaccines,^[21,26] the very low water-solubility of CAB and its high recommended dose (400 mg monthly) for IM administration) make MAP-mediated delivery challenging.

Herein we report, for the first time, the development of an innovative, stable, dissolving bilayer MAP with unique design and formulation prepared from biocompatible polymers for high-dose, long-acting micro-depot delivery of CAB for potential HIV PrEP (Figure 1).

2. Results and Discussion

2.1. Development and Fabrication of MAP Design

To maximize CAB intradermal (ID) delivery, we developed a unique MAP design with high needle density and superior insertion capability in the skin via careful selection of geometry.^[27] Our MAP (Figure 2A) has a baseplate with a total surface area of $\approx 0.5 \text{ cm}^2$ bearing 16×16 extended pedestal needles. Each extended pedestal needle consisted of a cuboidal base measuring $300 \mu\text{m}$ in height and $300 \mu\text{m}$ in width, with a pyramidal

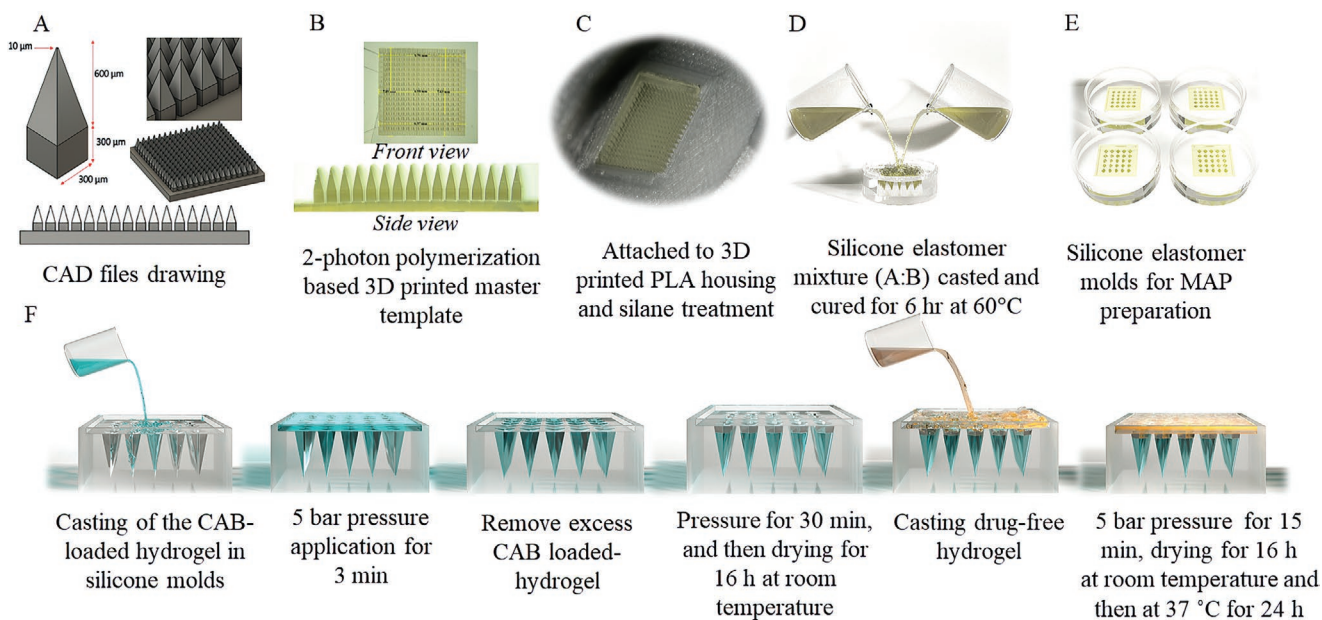


Figure 2. Representative images of A) CAD-assisted new design of MAP consisted of 16×16 extended pedestal needles. B) 3D printed MAP master template. C) MAP master template attached to polylactic acid [PLA] holder. D) A process of casting a mixture of LSR 9-9508-30 silicone elastomer mix (part A: part B, 1:1, w/w). E) MAP female mold prepared from PDMS. F) A schematic representation for the manufacturing procedures of a bilayer CAB-MAP, namely either CAB LA-MAP, CAB Na-MAP, or CAB FA-MAP.

tip measuring $600 \mu\text{m}$ in height. The needle tip radius is $10 \mu\text{m}$ to facilitate skin insertion. The needle-side to needle-side interspacing is $100 \mu\text{m}$ at the baseplate.

Our MAP design allowed relatively high needle density (256 needles per 0.5 cm^2 array), with the intention of enhancing penetration depth while avoiding the “bed of nails effect”.^[28] The pyramidal tip length/width aspect ratio (2:1) was chosen to attain sufficient mechanical strength and potential for deep insertion into the skin.^[28–30] Additionally, this MAP design should facilitate MAP demolding without needle breakage,^[28–30] thus enabling mass production of defect-free MAP. Based on our design and methods of production, needle length could be extended further. However, in practice, it is difficult to remove dissolving MAP needles longer than 1 mm from their mold, and the insertion of longer needles may cause pain and reduce acceptability and potential adherence.^[28]

The concept of the extended pedestal MAP is not new and was first reported by Chu et al.^[28] However, in their MAP design, the number of needles per array was limited to 100 needles per 0.5 cm^2 and needle tip insertion depth was limited to $\approx 40\%$ of their $600 \mu\text{m}$ length. This may be ascribed to the differences in the width of the cuboidal base and the side length of the base of the pyramidal tip ($340 \mu\text{m}$ vs $300 \mu\text{m}$).

Our MAP design (Figure 2A) was created by computer-aided design (CAD) software and used high-resolution 3D printing technology to fabricate its male master template from a relatively cheap resin,^[31] which was then used to create numerous sturdy, reusable poly(dimethyl siloxane) [PDMS] molds, as depicted in Figure 2B–E. These were employed to manufacture hundreds of bilayer MAP. Using such simple yet flexible technology could facilitate cost-effective and rapid transfer of MAP for mass production by industry.

2.2. Fabrication of Bilayer CAB-MAPs

Conventional dissolving MAPs are generally designed to deliver low doses of potent hydrophilic drugs into the skin.^[22,32] The amount of drug delivered usually depends on the amount of drug embedded within the MAP needles, in addition to drug diffusion from the backing layer (the baseplate) after MAP needle insertion. In this exploratory MAP study, a high dose of the poorly water-soluble solid particulate CAB should be delivered from a MAP size no bigger than conventional transdermal patches ($10\text{--}40 \text{ cm}^2$) for future human use. For such poorly water-soluble particulate drugs, only drug molecules loaded into the parts of the MAP needles that insert beneath the stratum corneum are likely to be deposited in the viable skin layers, and this means any baseplate-loaded drug will be wasted.^[32] Thus, CAB-MAP should be formulated with high drug loading into MAP needle tips only.

Polymers selected for high-drug-content dissolving MAP should: i) be water-soluble and biodegradable or biocompatible with $\text{MW} < 60 \text{ kDa}$, so that they are safe and can be eliminated from the body readily following skin deposition, ii) be compatible with CAB, so they do not cause particles aggregation or chemical instability, iii) produce a MAP with maximal drug loading while maintaining acceptable mechanical properties, iv) can achieve programmed dissolving (fast dissolving drug-loaded needle tips and slowly dissolving baseplate) so that the needle tips completely dissolve in $< 30 \text{ min}$ post skin insertion, to minimize MAP wear time. The backing layer should be slowly dissolving so that it can be removed intact without depositing an unpleasant gluey mass on the skin surface.^[33,34]

First, bilayer MAP was fabricated using the proprietary CAB LA nanosuspension after being concentrated (Section S1,

Supporting Information). Following a comprehensive formulation rationalization study, a hydrogel composed of poly(vinyl alcohol) (PVA) 10K (MW = 9–10 kDa)/poly(vinyl pyrrolidone) (PVP) (MW = 58 kDa) (20%: 20%, w/w) mixed with CAB LA (60% w/w, calculated based on tip dry weight) was used to form MAP tips (Section S2, Supporting Information). A drug-free hydrogel composed of PVA 50K (MW = 31–50 kDa)/PVP (MW = 58 kDa) (15%: 20%, w/w) was employed to form the second MAP layer (the cuboidal bases and the baseplate), also called the backing layer (Section S3, Supporting Information). These two polymeric blends mixed at the aforementioned optimized ratios generated mechanically strong MAP, which could be ascribed to the synergistic effect of mixtures between PVA and PVP and formation of hydrogen bonds between the carbonyl groups of PVP and hydroxyl groups of PVA that improves the polymeric blend crystallinity and cohesiveness,^[35–38] with programmed dissolution (fast-dissolving tips and slow-dissolving backing layer) features.

These two hydrogels were also used to fabricate bilayer MAPs from the less expensive micronized forms of the drug, that is, CAB Na (the finalized CAB Na-MAP) and CAB FA (the finalized CAB FA-MAP), with equal drug loading (Section S4, Supporting Information) in order to investigate their potential use as cost-effective alternatives to the proprietary CAB LA nanosuspension in MAP fabrication. Using a combination of PVA and PVP was also highly beneficial in producing homogenous CAB microparticulate loaded-hydrogel with sufficiently strong MAP tips. This could be attributed to the surface activity of those two polymers and their ability to improve drug microparticles wettability and homogenous distribution within the hydrogel.

Both PVA and PVP are inexpensive polymers and generally regarded as safe substances by the US FDA and have excellent profiles in terms of low toxicity and biocompatibility.^[39–42] Additionally, PVP is used as a plasma expander.^[43] Both PVA and PVP with MW <60 kDa are known to be readily eliminated from the body by the kidneys.^[44,45] Indeed, PVA 10K has a very short apparent plasma half-life, ≈ 90 min.^[45] Thus, both polymers can be considered safe and are unlikely to accumulate in the body once deposited in the skin post MAP dissolution.

In general, dissolving MAP can be prepared by various micro-molding methods, including the conventional centrifuge method,^[35,46] the roller method,^[47] or a positive pressure chamber.^[48] Here, the positive pressure chamber method was adopted and rationalized to produce our bilayer MAP via a simple two-step process, as depicted in Figure 2F. Briefly, the drug-loaded hydrogel for the MAP tips was first cast, and excess hydrogel then removed and dried. Subsequently, the drug-free hydrogel was cast to form the second MAP layer. Bilayer MAPs were then dried and demolded for further characterization. This manufacturing method is simple, potentially cost-effective and scalable for mass production, which could streamline the transition of MAP from laboratory scale to industry and subsequent commercialization.

In the following sections, we report the results of in vitro, ex vivo characterization and the in vivo performance, safety, and tolerability of the finalized CAB-MAPs, namely CAB LA-MAP, CAB Na-MAP, and CAB FA-MAP.

2.3. CAB-MAPs In Vitro Characterization

2.3.1. CAB-MAPs Physical Characterization

To ensure successful production of defect-free bilayer MAP structures with the specified geometry from the three drug forms, the finalized CAB-MAPs were inspected using a light microscope and scanning electron microscope (SEM). Representative light microscope images (Figure 3A) showed that bilayer MAP structures with sharp tips and smooth surfaces were formed, irrespective of the drug form used. This was also confirmed by SEM images (Figure 3B), where CAB LA-MAP and CAB Na-MAP appeared to have smooth surfaces (Figures 3B(i),(ii), respectively), which is mainly due to the nano-sized particulates of CAB LA and amorphous structures of CAB Na. In contrast, CAB FA-MAP exhibited a rough surface (Figure 3B(iii)), because of large micron-sized, poorly water-soluble particulates of CAB FA. Upon measuring the MAPs' needle dimensions, they were found to be consistent with the geometry of the master template, apart from a trivial shrinkage ($\approx 5.5\%$) in the needle length, which measured ≈ 850 μm (the length of the cuboidal base and pyramidal tip were ≈ 250 μm and ≈ 600 μm , respectively), which can be attributed to the contraction of the polymeric matrix upon drying.^[35,42]

2.3.2. Evaluation of the Effect of MAP Polymers and Fabrication Process on Drug Physical Stability and Distribution in MAP Polymeric Matrix

Maintaining the physical stability of the poorly water-soluble drug particulates, specifically as monodispersed systems, within the MAP polymeric matrix is crucial to maintain the drug's ability to be released in a controlled and consistent fashion.^[32,37] Additionally, the homogeneous distribution of drug particulates within the polymeric matrix is of paramount importance for MAP mechanical strength and consistent dosing.^[32,37,49] Therefore, drug physical stability and distribution in the polymeric matrix after its incorporation into MAP tips were investigated by employing SEM, x-ray diffractometer (XRD), differential scanning calorimetry (DSC), dissolution kinetics in phosphate buffer saline (PBS), and particle size analysis.

Representative SEM images of cross-sectioned CAB-MAP tips (Figure 3C) in the three finalized CAB-MAPs showed that the drug was homogeneously embedded within the polymeric matrix as monodispersed systems, and no aggregates could be observed. This finding was confirmed upon CAB-MAPs dissolution in PBS (Section S5, Supporting Information), where drug particles appeared as monodisperse systems and no drug aggregates could be observed post MAPs dissolution. Particle size and polydispersity index (PDI) of CAB LA recovered from bilayer CAB LA-MAPs were shown to be ≈ 404 nm and ≈ 0.172 , respectively, which were slightly increased, but they were still within the same range as those reported for CAB LA before its incorporation into the MAP matrix (≈ 342 nm and ≈ 0.182 , respectively).

XRD analysis also showed that the three CAB forms incorporated within the MAPs' polymeric matrices exhibited

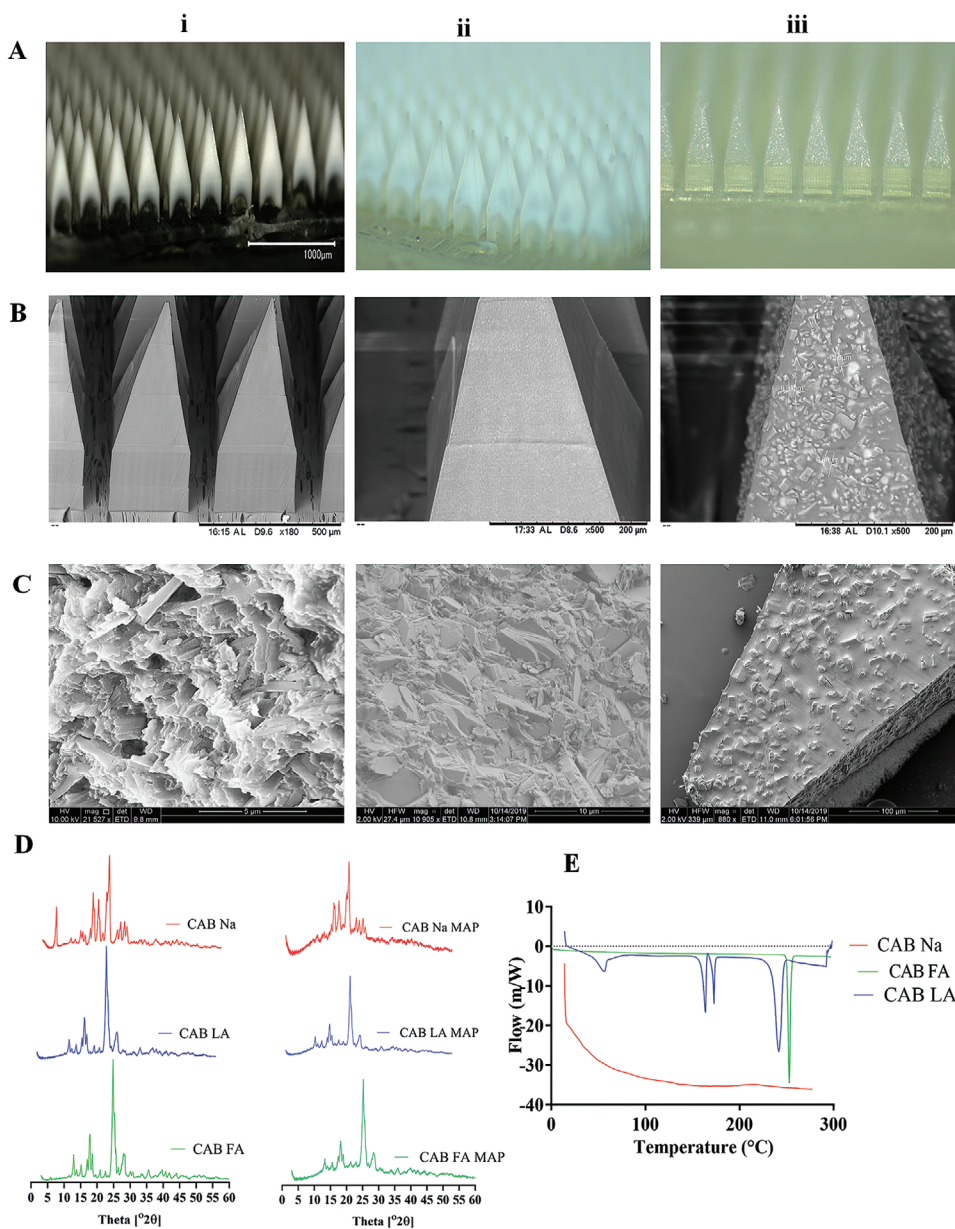


Figure 3. Representative A) light microscope and B,C) SEM images of the finalized bilayer i) CAB LA-MAP, ii) CAB Na-MAP, and iii) CAB FA-MAP, respectively. D) XRD diffractograms of the three forms of CAB before and after their incorporation in the first MAP layer polymeric matrix. E) DSC thermograms of the three forms of CAB.

XRD diffractograms comparable to those exhibited by their unformulated pure drug counterparts (Figure 3D), where both CAB FA and CAB LA were shown to possess crystalline structures, but CAB Na was amorphous. These were consistent with the results of DSC analysis (Figure 3E), where CAB LA and CAB FA exhibited sharp endothermic peaks at 236 and 249 °C, respectively, confirming their crystalline structures. However, CAB Na showed no peaks, confirming its amorphous structure. These results suggest that MAP matrix polymers and the fabrication process had no meaningful effect on the physical stability of the three-drug forms, which were homogeneously distributed within the matrix as monodisperse systems.

2.3.3. CAB MAPs Drug Content

The amount of drug loaded into the MAP tips has a significant impact on the dose delivered into the skin.^[42,49] Therefore, we measured the drug content of the three finalized CAB-MAPs by dissolving them in deionized (DI) water and then quantifying the drug in the resultant solution using a validated high-performance liquid chromatography coupled with ultraviolet detector (HPLC-UV) method. To ensure that the quantified drug was tip-localized and did not come from the baseplate, we also calculated the theoretical drug content of CAB-MAP tips based on the total tip volume ($\approx 4.61 \mu\text{L}/\text{MAP}$) and density in the dry state ($\approx 1.11 \text{ mg mm}^{-3}$) (Section S6, Supporting Information). Results

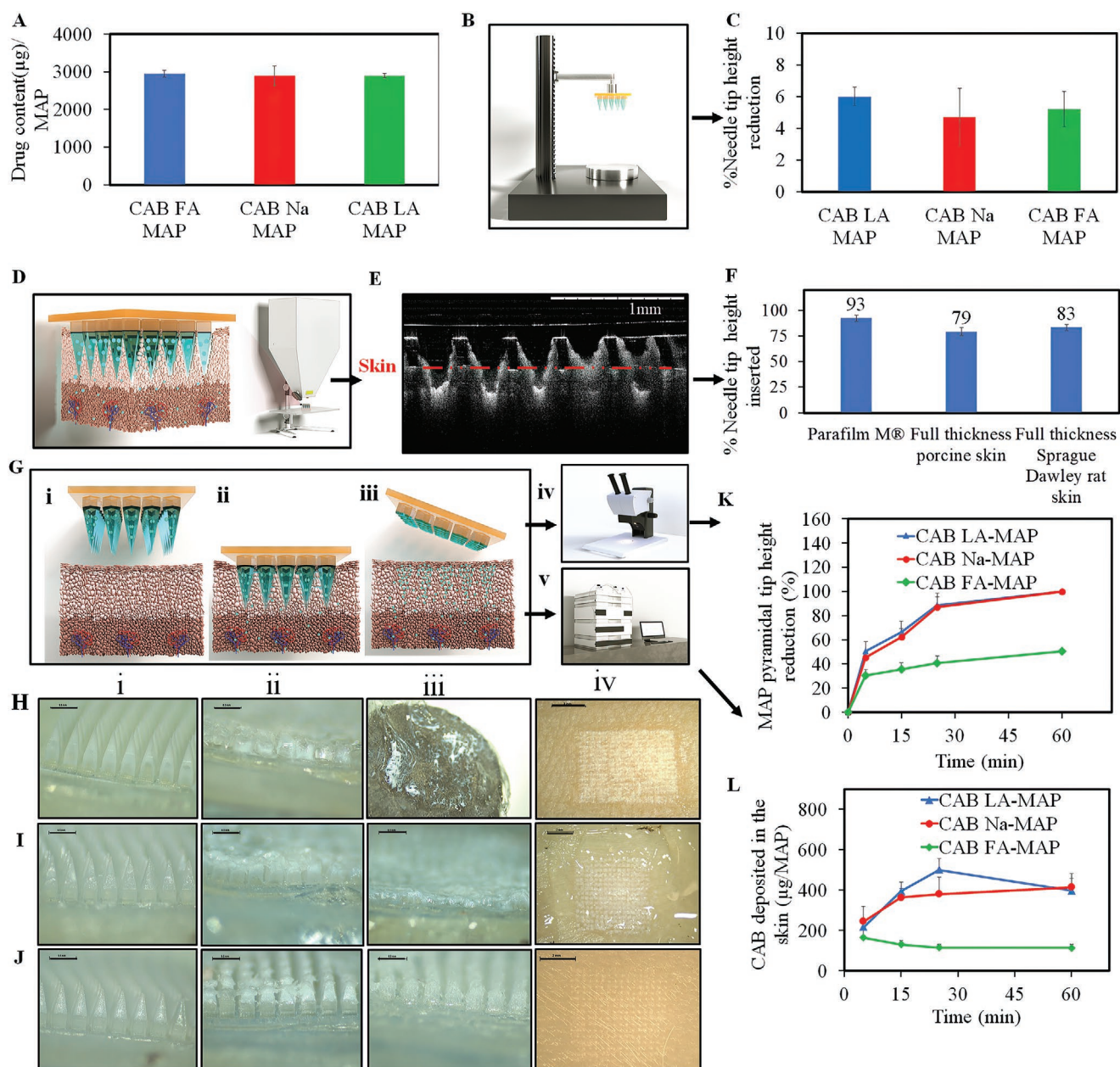


Figure 4. A) Drug content of the finalized bilayer CAB-MAPs ($\mu\text{g}/0.5 \text{ cm}^2$ MAP). B) Schematic representation for the experimental setup for the mechanical testing of CAB-MAPs. C) Percentage of reduction of needle height of the finalized CAB-MAPs upon applying a compression force of 32 N for 30 s against the aluminum block. D) Schematic representation of skin application of CAB-MAP and OCT equipment. E) Representative OCT images for CAB LA-MAP after insertion into porcine skin. F) Percentage of CAB LA-MAP needle tip height that inserted into a stack of 8 layers of Parafilm M, excised full-thickness neonatal porcine skin, and rat skin, respectively. Data are reported as means \pm SD, $n = 3$. G) Schematic illustration of skin deposition study. H–J) Representative light microscope images of the finalized bilayer MAPs containing H) CAB LA-MAP, I) CAB Na-MAP, or J) CAB FA-MAP, respectively, after insertion into excised full-thickness neonatal porcine skin for predetermined time intervals of i) 0 min, ii) 25 min, and iii) 60 min, and iv) light microscope images of skin after CAB deposition at $32 \pm 1 \text{ }^\circ\text{C}$. K) The percentage of height reduction of MAP tips of either of the finalized bilayer CAB-MAPs after insertion into an excised full-thickness neonatal porcine skin for predetermined time intervals at $32 \pm 1 \text{ }^\circ\text{C}$. L) The amount of drug ($\mu\text{g}/0.5 \text{ cm}^2$ MAP) deposited in excised full-thickness neonatal porcine skin post insertion of the finalized bilayer CAB-MAPs for predetermined time intervals at $32 \pm 1 \text{ }^\circ\text{C}$.

showed that the measured drug content of the finalized CAB-MAPs was almost identical (Figure 4A) and was $\approx 3000 \mu\text{g}/\text{MAP}$, which was not significantly ($p < 0.05$) different from the theoretically calculated drug content ($\approx 3100 \mu\text{g}/\text{MAP}$). This further

confirms that the loaded drug was mainly localized in the MAP tips. Such tip-localized drug loading in a relatively small MAP (0.5 cm^2) represents a remarkable increase in loading capacity compared to previously reported other MAP types.^[28,32,50]

2.3.4. CAB-MAPs Mechanical and Insertion Properties

This study aimed to evaluate the mechanical and insertion properties of the finalized CAB-MAPs, as these will be critical to their successful use in the clinic.^[42,49] Essentially, MAP tips should have sufficient mechanical strength to withstand a compression force of 32 N per MAP, which has been shown to be the maximum force applied by volunteers manually inserting MAPs into their own skin,^[51] to achieve sufficiently deep insertion in the skin to deliver the highest possible amount of the tip-loaded drug.^[42,49] These properties were evaluated using a commonly used and validated method employing a texture analyzer.^[52] To assess their mechanical properties, a MAP was attached to the probe of the texture analyzer and compressed against an aluminum block for 30 s (Figure 4B), after which the percentage needle height reduction was determined. Results (Figure 4C) showed that the finalized CAB-MAPs exhibited almost identical height reduction (between ≈ 4.7 and $\approx 6.0\%$), which could be considered inconsequential.^[53] Importantly, microscopic inspection of all tested MAPs showed that compression of the needles starts from the tapered tip and all needles maintained their out-of-plane structure, with no cracks observed at the base or tips. Previous studies showed that MAPs that encountered up to 20% reduction in height were still successfully inserted into the skin, *in vitro* and *in vivo* settings.^[48,52,54] This suggests that the finalized CAB-MAPs possess satisfactory mechanical properties to withstand normal handling and skin insertion.

To assess the insertion properties of the finalized CAB-MAPs, the same experimental setup as the mechanical property test was used. However, to get a good insight into how they would behave upon insertion into human skin, MAPs were applied to validated skin models, including Parafilm M,^[53] neonatal porcine skin, which is a common surrogate for human skin,^[55] and Sprague Dawley rat skin. Since the insertion capability of a MAP is dependent on MAP geometry and mechanical properties,^[51,52] and the finalized CAB-MAPs exhibited very similar mechanical properties. The finalized CAB LA-MAP insertion properties were evaluated as a representative. The percentage of MAP tip height that inserted in three skin models was determined using optical coherence tomography (OCT) (Figure 4D), which is an excellent non-invasive tool that is widely used to accurately measure the insertion depth of MAP needles.^[37,53] OCT image (Figure 4E) clearly showed that MAP tips were well-inserted in the skin models. The calculated percentage of MAP pyramidal tip height ($\approx 600 \mu\text{m}$) that inserted in the three skin models (Figure 4F) were found to be of the magnitude of $\approx 93\%$, $\approx 79\%$, and $\approx 83\%$, respectively, indicating excellent insertion capability. The achieved insertion with such high needle density represents a meaningful improvement in comparison with many previously reported MAP designs with a comparable surface area, such as 14×14 MAP ($\approx 60\%$ of the height of $600 \mu\text{m}$ the needles inserted in Parafilm M),^[49] 19×19 MAP ($\approx 50\%$ of the height of $600 \mu\text{m}$ needles inserted in Parafilm M), or 11×11 MAP ($\approx 65\%$ of the height of $600 \mu\text{m}$ needles inserted in Parafilm M),^[56] or even 10×10 extended pedestal MAP ($\approx 40\%$ of the height of $600 \mu\text{m}$ needle tips inserted in porcine skin.^[28] Results from both tests demonstrate that the finalized CAB-MAPs have sufficient mechanical strength and insertion

capabilities, thus suggesting their potential use for efficient ID delivery of CAB in humans.

2.4. CAB-MAPs Dissolution Kinetics and Drug Deposition in the Skin (Ex Vivo)

Moving further with the finalized CAB-MAPs, dissolution kinetics and drug deposition studies were performed to estimate the wear time by which MAP tips would be dissolved and have deposited their payload in the skin and to determine MAP delivery efficiency. Such properties are crucial for future use and may influence the required patch size and frequency of administration, as well as potential patient adherence. In theory, the shorter the wear time the better for patient adherence.^[33,52,57] Also, the higher the delivery efficiency, the smaller the patch size, which may affect manufacturing scale-up and ease of use by patients. To mimic their application to human skin, the finalized CAB-MAPs were applied to excised full-thickness neonatal porcine skin (Figure 4G), which is a good model for human skin,^[55,58] using the fingertips and left in place for predetermined time intervals (5, 15, 25, and 60 min and 24 h). The MAPs were inspected before and after application by light microscopy (Figure 4G(iv)) to determine the percentage height reduction of MAP tips (due to dissolution in the skin) versus time. The skin at the application site was then meticulously cleaned, inspected by light microscope, and subsequently biopsied and analyzed for drug content to determine the amount of drug delivered by the MAPs for each “wear time” (Figure 4L).

Results showed that both CAB LA-MAP and CAB Na-MAP displayed almost identical dissolution profiles (Figure 4K). As it can be seen in the Figure 4H,I, respectively), both MAP tips started dissolving within 5 min (the first sampling point) post skin insertion (Figure 4H(i),I(i)), with $\approx 50\%$ being dissolved, and then MAP tips continued dissolving rapidly to reach $\approx 90\%$ and $\approx 100\%$ after 25 and 60 min, respectively (Figure 4H(ii and iii),I(ii and iii)). Interestingly, the MAP baseplates were removed intact, even after 60 min post MAP application (Figure 4H(iii),I(iii), respectively). Applying MAPs for 24 h resulted in complete MAP dissolution, including tips and baseplates, forming a whitish glue-like mass consisting of undelivered drugs and the dissolved polymers (images are not shown). In contrast, CAB FA-MAP dissolved slowly in the skin (Figure 4K,J)(i,ii,iii), and only $\approx 40\%$ of the MAP tips dissolved within 60 min post MAP application. Again, complete MAP dissolution occurred by 24 h. This suggests that 60 min application time for the MAPs containing CAB LA or CAB Na would be sufficient for the MAP tips to completely dissolve in the skin while the baseplate remains intact, facilitating removal. However, a longer wear time (>60 min) would be needed for CAB FA-MAP.

These variations in dissolution profiles between CAB LA-MAP, CAB Na-MAP, and CAB FA-MAP may be ascribed to the smaller particle size and enhanced solubility of nano-sized CAB LA and amorphous CAB Na compared to CAB FA, which has micron-sized poorly water-soluble particles that potentially affected the wettability and dissolution of the MAP tips in the skin interstitial fluid. The short dissolution time (<60 min) exhibited by both CAB LA-MAP and CAB Na-MAP represents

a notable decrease in the dissolution time of drug-loaded tips in comparison with other previously reported studies for a very hydrophobic drug (rilpivirine), in which the required time for dissolution of the drug-loaded tips was ≈ 5 h.^[49]

Concerning drug deposition achieved by three finalized CAB-MAPs, the light microscope images of the skin at the application sites (Figure 4H(iv),I(iv),J(iv), respectively), clearly showed MAP tips deposited in the skin underneath the stratum corneum, which appeared like hundreds of whitish microdots for both CAB LA-MAP and CAB Na-MAP, indicating a relatively high amount of drug being deposited in the skin. In contrast, CAB FA-MAP produced relatively small, faded white-colored dots suggesting a reduced amount of drug being deposited in the skin. This was consistent with the results of drug analysis in the harvested skin samples (Figure 4L), which revealed that both CAB LA-MAP and CAB Na-MAP achieved the highest drug deposition, which was of the magnitude of ≈ 499.6 $\mu\text{g}/\text{MAP}$ ($\approx 16.9\%$ of the loaded dose per MAP) and ≈ 413 $\mu\text{g}/\text{MAP}$ ($\approx 14.5\%$ of the loaded dose per MAP), respectively. These were obtained at 25 min post MAP application; no significant increase ($p > 0.05$) in amounts of drug deposited in the skin was observed for longer wear times, indicating that 25 min may be sufficient for MAP tips to be dissolved to deliver the maximum amount of drug. On the other hand, CAB FA-MAP showed significantly ($p > 0.05$) decreased drug deposition capability in comparison with the other two CAB-MAPs, where the amount of drug deposited in the skin post 24 h application was of the magnitude of ≈ 225.5 $\mu\text{g}/\text{MAP}$ (7.7% of the loaded dose per MAP). This may be ascribed again to its poor water-solubility, compounded by its micron-sized particles.

The delivered drug amount by the three finalized CAB-MAPs was, indeed, significantly ($p > 0.05$) lower than we expected based on drug loading, considering the exceptional insertion capability of our MAP tips in the skin models. This could be attributed to the hydrophobic nature of the drug and skin elasticity, manifested as an ability to stretch by up to 200 μm before being pierced by the MAP tips.^[29,30] This could mean that the upper parts of the pyramidal tips, which contain the highest proportion of drug, do not go beneath the stratum corneum but instead reside with these micron-scale “skin folds”, preventing more efficient drug deposition in the viable skin layers. However, although the percentage deposition of CAB LA and CAB Na were below our expectations considering the attained insertion, the mass of the drug deposited in each case still represents a remarkable achievement for such a hydrophobic drug. Indeed, delivery of similarly high doses of compounds with such properties have never been attained before.^[28,50,59–61]

2.5. CAB LA-MAP Stability Studies

The stability of MAPs is a crucial aspect for their development and moving forward to commercialization. Therefore, we conducted a stability study, using the finalized CAB LA-MAP as a representative, at two storage testing conditions; intermediate or accelerated for 6 months, as per the International Conference for Harmonisation guidelines.^[62] Results (Section S7, Supporting Information) revealed that the finalized CAB LA-MAP was stable at both storage conditions.

2.6. In Vivo Studies

The results from the in vitro and ex vivo characterization revealed that the finalized bilayer CAB-MAPs, namely CAB LA-MAP, CAB Na-MAP, and CAB FA-MAP, were promising, as they were stable, mechanically strong, and able to deliver substantial amounts of CAB into ex vivo skin. However, these findings need to be complemented by in vivo data to evaluate the performance (pharmacokinetics [PK]), safety, and tolerability of the finalized CAB-MAPs following single and repeated dosing using healthy female Sprague Dawley rats, a good preclinical model for screening and evaluating the PK of long-acting formulations.^[63] For comparison, rats received the proprietary CAB LA nanosuspension by IM injection (the conventional administration route) or by ID injection (to evaluate the effect of the anatomy and physiology of the skin). Studies details were reported in (Section S8, Supporting Information).

To facilitate translating our in vivo findings to human application, while accounting for the biological and anatomical differences between humans and rats and the fact that rats eliminate drugs faster than humans,^[64] allometric scaling (Section S9, Supporting Information) was used to calculate the monthly dose for rats based on a human monthly dose of 400 mg (equates to 5.71 mg/kg in a person with an average body weight of 70 kg).^[13] This was found to be ≈ 40 mg/kg (equates to 10 mg/rat, for a rat with an average body weight of 250 g).^[64]

2.6.1. CAB Pharmacokinetics After a Single Dose of CAB-MAPs

As the first step in MAP performance assessment, this study was designed i) to evaluate MAP's functionality in vivo (the ability of the finalized CAB-MAP tips to be inserted in the skin, dissolved, and have deposited their payload); ii) to evaluate how the skin anatomy and physiology (where MAPs are expected to deliver their payload) would affect CAB PK in comparison with IM injection; iii) to estimate MAP delivery efficiency and absorption rate and assess whether the three drug-forms—namely CAB LA, CAB Na, or CAB FA—delivered by MAPs would achieve long-acting PK profiles that maintain drug plasma levels above the effective therapeutic concentration in humans over a 4-week period (to mimic human monthly dosing) in a similar fashion to IM injection (the conventional administration route). The effective therapeutic concentration in humans that provides 100% protection against HIV-1 was reported to be 0.664 $\mu\text{g mL}^{-1}$, which is equivalent to four times the protein-adjusted 90% inhibitory concentration ($4 \times \text{PA-IC}_{90}$).^[65]

To this end, five cohorts of rats were assigned to this study, as illustrated in Figure 5A. In the first two cohorts, each rat received CAB LA (10 mg/rat) by either IM injection (cohort 1) or ID injection (cohort 2). The other three cohorts (3–5) were allocated for MAP application. In these three cohorts, each rat received the drug by simultaneous application of $4 \times$ MAPs of either the finalized CAB LA-MAP (cohort 3), CAB Na-MAP (cohort 4), or CAB FA-MAP (cohort 5) for 24 h. The skin at MAP application sites was imaged post MAPs remaining removal (after 24 h from the application) using a digital camera and inspected for evidence of drug delivery and any sign of

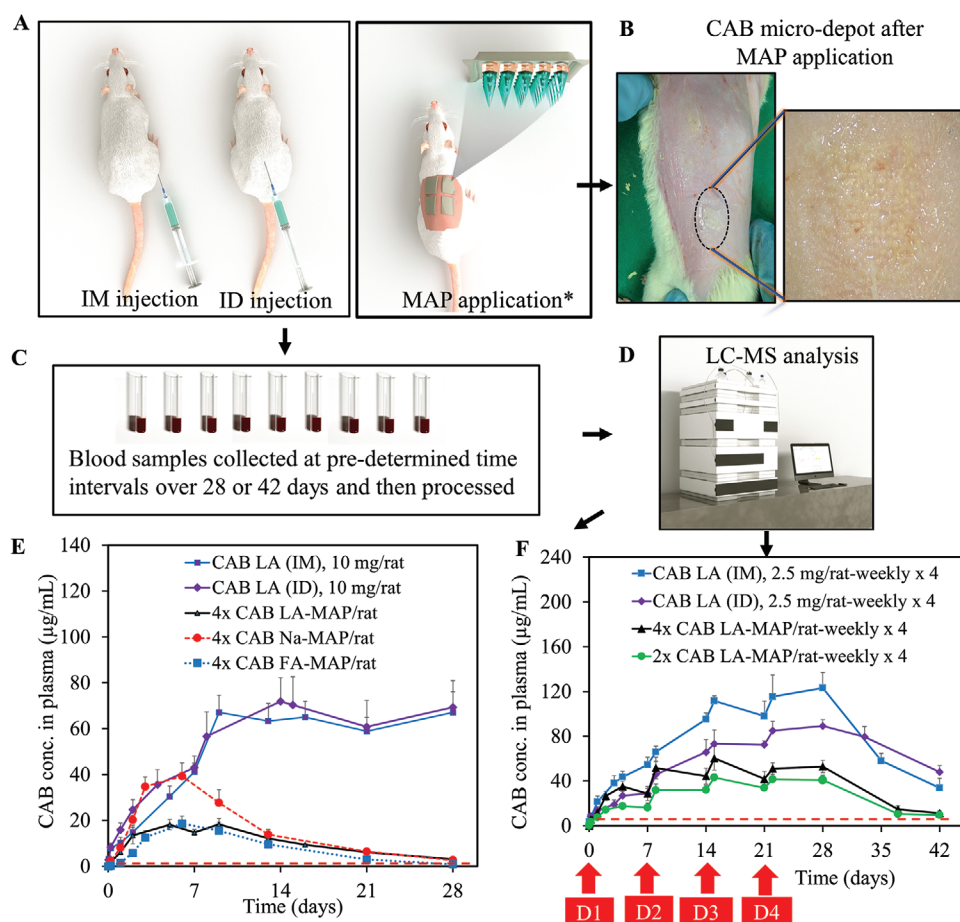


Figure 5. A) Schematic representation of the in vivo experimental setup [* For single dose, three cohorts were allocated to receive the drug by simultaneous application of 4× patches of either the finalized CAB LA-MAP, CAB Na-MAP, or CAB FA-MAP. For repeated dose, two cohorts were allocated to receive the drug by simultaneous application of either 4× patches or 2× patches of the finalized CAB LA-MAP]. B) Exemplar digital images of rat skin at the application site upon removal of CAB LA-MAP post-24 h application with visible whitish micro-depots representing MAP tips implanted in the skin. C) Schematic diagram representing blood collection from rats at predetermined time intervals over studies periods. D) Schematic illustration of LC-MS setup used. E) CAB PK profiles post administration of a single dose of CAB LA either by IM injection or ID injection or applying 4× CAB LA-MAP (containing ≈11.72 mg CAB LA in total), 4× CAB Na-MAP (containing ≈11.0 mg CAB Na in total), or 4× CAB FA-MAP (containing ≈11.8 mg CAB FA in total). F) CAB PK profiles post administration of a repeated once-weekly × 4 doses of CAB LA (2.5 mg/rat) by IM injection or ID injection or applying 4× or 2× CAB LA-MAP (containing 11.72 or 5.86 mg in total, respectively). Red dotted lines in (E) and (F) indicate the minimum therapeutic plasma levels for PrEP ($4 \times \text{PA-IC}_{90} = 0.664 \mu\text{g mL}^{-1}$). Data are reported as means ± SD, $n \geq 5$.

toxicity or irritation (Figure 5B). Blood samples were collected from all cohorts at predetermined time intervals over 28 days (Figure 5C) and assayed for CAB content by a validated UPLC-MS-MS method (Figure 5D) (Section S10, Supporting Information). Data were then used to construct the mean CAB plasma concentration versus time profiles, which were then used to calculate the key PK parameters (Section S11, Supporting Information), including the maximum drug concentration (C_{max}), the time of maximum concentration (T_{max}), the apparent half-life ($t_{0.5}$), and drug minimum concentration (C_{trough}), that is, (C_{28}) at day 28. The area-under-the-curve from time zero ($t = 0$) to the last experimental time point ($t = 28$ days) (AUC_{0-28}) and the dose/body weight normalized PK parameters (specifically C_{max} and AUC_{0-28}) (Table 1) were used for comparison with their corresponding PK parameters achieved by administering the drug by IM injection. Finally, the relative bioavailability (FR) in comparison with IM injection was also calculated and reported.

Furthermore, conducting such a comprehensive study necessitated using a considerable number of rats and performing the experiment in multiple steps, which resulted in inevitable inter-cohort weight variations. Due to the difficulty of tailoring the administered dose as per rats' weights, a fixed dose (assuming a rat's average weight to be ≈250 g) was given to each rat as per cohort, which resulted in inter-cohort dose/body weight (calculated as mg/kg) disparity. To eliminate the effect of the inter-cohort dose/body weight (mg/kg) disparity among the cohorts of interest, weight-dependent PK parameters, specifically drug concentrations (C) and the area-under-the-curve (AUC), were normalized (Section S11, Supporting Information) and reported.

Inspecting skin at application sites (Figure 5B) in all rats (cohorts 3–5) showed that, post-application for 24 h, all MAPs completely dissolved, forming a whitish gluey mass consisted of the undelivered drug and the dissolved polymers from the

Table 1. CAB PK parameters in Sprague Dawley rats and their corresponding dose/body weight-normalized counterparts following administration a single dose of either CAB LA, CAB Na, or CAB FA by either IM or ID injection or MAP application. Data are reported as mean \pm SD, $n \geq 5$.

Cohort no.	Drug form used/ admin. route	Dose [mg/kg]	Experimental PK parameters					Dose/body weight (as if 40 mg/kg is given) normalized PK parameters	
			T_{max} [days]	$t_{0.5}$ [days]	C_{max} [$\mu\text{g mL}^{-1}$]	AUC_{0-28} [$\mu\text{g}\cdot\text{day mL}^{-1}$]	C_{28} [$\mu\text{g mL}^{-1}$]	norm- C_{max} [$\mu\text{g mL}^{-1}$]	norm- AUC_{0-28} [$\mu\text{g}\cdot\text{day mL}^{-1}$]
1	CAB LA/IM	35.9 (± 4.5)	9	–	67.1 (± 7.6)	1472.5 (± 150.0)	67.1 (± 9.1)	74.7 (± 8.6)	1637.6 (± 167.2)
2	CAB LA/ID	50.2 (± 4.0)	14	–	71.9 (± 10.4)	1459.8 (± 324.2)	69.4 (± 15.8)	57.3 (± 8.3)	1163.2 (± 258.3)
3	CAB LA-MAP	35.3 (± 2.4)	5	7.3	18.1 (± 2.3)	291.1 (± 23.4)	3.1 (± 1.1)	20.5 (± 2.6)	329.8 (± 26.5)
4	CAB Na-MAP	59.3 (± 1.8)	6	5.8	39.3 (± 5.8)	454.3 (± 23.4)	2.7 (± 0.4)	26.5 (± 3.9)	306.5 (± 15.8)
5	CAB FA-MAP	61.0 (± 2.1)	6	4.5	18.7 (± 3.2)	226.3 (± 13.4)	0.9 (± 0.7)	12.4 (± 2.1)	148.4 (± 8.8)

baseplates (images are not shown). After a meticulous cleaning, hundreds of whitish microdots were revealed to be deposited in the skin (Figure 5B), which comprised the implanted MAP drug-loaded tips in the skin. This observation was consistent with the findings of ex vivo drug deposition studies reported in the previous section, confirming the functionality of the finalized CAB-MAPs in an in vivo setup.

Regarding the effect of skin anatomy and physiology of CAB PK in comparison with IM injection, we studied the CAB PK profiles produced by ID injection and compared them to those produced by IM injection. In those rats that received CAB LA by IM injection, the drug appeared in plasma within 1 h (the first sampling point) post-dosing and rapidly increased in concentration to reach $\approx 8.4 \mu\text{g mL}^{-1}$ at 4 h and then continued to increase gradually to reach its C_{max} ($67.1 \mu\text{g mL}^{-1}$) at T_{max} (9 days). Subsequently, drug concentrations continued fluctuating around C_{max} until day 28 (the end of the study period). This PK profile and parameters are very comparable to a previously reported CAB LA PK profile, where it was previously reported that $T_{max} = 7\text{--}14$ days and $C_{max} \approx 70.5 \mu\text{g mL}^{-1}$ upon administering a similar CAB LA dose (40 mg/kg) by IM injection to the same strain of rats.^[66] In those rats that received CAB LA by ID injection, the drug exhibited almost identical PK profiles, except the time ($T_{max} = 14$ days) to reach C_{max} ($71.0 \mu\text{g mL}^{-1}$). This time is significantly ($p < 0.05$) longer than that observed post IM injection. Upon comparing the normalized PK parameters (Table 1), specifically the norm- C_{max} ($\approx 573 \mu\text{g mL}^{-1}$), and norm- AUC_{0-28} ($\approx 1163.2 \mu\text{g}\cdot\text{day mL}^{-1}$), were found to be significantly lower ($p < 0.05$) and equate to ≈ 76.6 and $\approx 71.0\%$, respectively, of the corresponding PK parameters produced by IM injection ($\approx 74.7 \mu\text{g mL}^{-1}$ and $\approx 1637.6 \mu\text{g}\cdot\text{day mL}^{-1}$, respectively). Taking into consideration that ID-injected drug by the hypodermic needle can be completely delivered into the skin, it concluded that the longer T_{max} , and lower norm- C_{max} and norm- AUC_{0-28} , were not because of the decreased delivery efficiency but may be due to a decreased dissolution or absorption rate from the viable skin layers. This was not unexpected, taking into account the inherited structural physiological differences between the two tissues and the slower blood flow rate in the skin tissue, in comparison with blood flow in the muscles.^[67] Interestingly,

the PK profile of CAB post ID injection of CAB LA presented here was comparable to CAB PK profiles obtained post administering an equivalent dose of CAB LA to rats of the same strain by subcutaneous injection.^[66]

The PK profiles of CAB in the rats from the three cohorts (3–5) that received the three forms of the drug by MAPs (Figure 5E), showed that, similarly to IM injection, the drug appeared in plasma within 1 h of dosing and no lag time was observed. CAB plasma concentration then increased rapidly to achieve plasma levels 2.8-fold above $4\times$ PA-IC₉₀ after 4 h from dosing and continued increasing to achieve C_{max} at T_{max} (5 days for CAB LA-MAP and 6 days for the other two MAPs), indicating fast absorption rates from MAPs. Subsequently, the plasma levels fluctuated around C_{max} for a few days and then decreased gradually to reach (C_{28}) at day 28, which was MAP type-dependent, but was still above $4\times$ PA-IC₉₀ in all three cohorts.

The observed T_{max} (5 and 6 days) in those rats that received the drug by MAPs were significantly ($p > 0.05$) shorter than T_{max} post IM injection (9 days) or ID injection (14 days). This suggests that the drug absorption rate from MAP application sites was greater than that from IM and ID injected depots. This may be ascribed to the hundreds of micro-depots the MAP drug-loaded tips implanted in the skin, which will have considerably larger surface areas than the single “large” depot delivered by IM or ID injection using hypodermic needles.^[68] The higher absorption rate achieved by MAPs has a potential advantage, not only because it combats the slower absorption rate caused by the inherited physiology and anatomy of the skin, but also because it could help in quickly achieving the required drug plasma levels for immediate protection against HIV-1 infections.

In terms of MAP delivery efficiency, CAB plasma exposure (as exemplified by C_{max} and AUC_{0-28}) achieved by all CAB-MAPs were MAP type-dependent and significantly lower than that achieved by IM injection (Table 1), which is consistent with incomplete drug delivery by MAPs. This was not unexpected for such a hydrophobic drug, and indeed, it was in good agreement with our observation of the skin at MAP application sites (in vivo) and with the results of the ex vivo drug deposition

studies reported in the previous section. Accordingly, not all drugs encapsulated within the MAP tips would be expected to be delivered throughout the 24 h application time, unlike the complete delivery by IM or ID injection.

At this stage, it was very challenging to accurately calculate the relative bioavailability (FR) of the drug from MAPs in comparison with IM injection due to incomplete drug absorption from both IM and MAP cohorts over 28 days (the study period). However, assuming no significant differences in the drug absorption and elimination kinetics between the two administration routes, IM, or MAP, from day 28 and onward, we can still cautiously use the partial absorption data to calculate FR and then use it to perform estimation for the percentage of drug delivered by each MAP. Under this assumption, the FR of drugs from CAB LA-MAP, CAB Na-MAP, and CAB FA-MAP were of the magnitude 0.2, 0.19, and 0.09, respectively. Hence, the amount of drug delivered by 4× MAPs/rat would be of the magnitude of $\approx 0.585 \text{ mg/MAP} \times 4 \approx 2.340 \text{ mg}$ for CAB LA-MAP, $\approx 0.570 \text{ mg/MAP} \times 4 \approx 2.280 \text{ mg}$ for CAB Na-MAP, and $\approx 0.270 \text{ mg/MAP} \times 4 \approx 1.080 \text{ mg}$ for CAB FA-MAP, respectively. This suggests that both CAB LA-MAP and CAB Na-MAP exhibited a comparable relative bioavailability that was almost twice that achieved by CAB FA-MAP. This finding is consistent with *in vivo* observation and in good agreement with the results of the *ex vivo* drug deposition study reported in the previous section.

Interestingly, despite the incomplete drug delivery by MAPs, the delivered doses rapidly achieved plasma levels that were maintained above 4× PA-IC₉₀ throughout the 28-day study period, indicating long-acting PK profiles achieved by the applied CAB-MAPs. This was evident from the achieved (C_{28}) at day 28 by CAB LA-MAP, CAB Na-MAP, and CAB FA-MAP, which were of the magnitude ≈ 3.1 , ≈ 2.7 , and $\approx 0.9 \mu\text{g mL}^{-1}$, respectively. These are ≈ 4.7 , ≈ 4.1 , and ≈ 1.4 -fold, respectively, above the 4× PA-IC₉₀.

The comparable C_{28} achieved by CAB LA-MAP and CAB Na-MAP, which are several-fold higher than that achieved by CAB FA-MAP, could be due to the relatively high delivery efficiency achieved by those two MAPs.

These findings are very encouraging and demonstrated the functionality of these MAPs in rats. However, in order to predict MAP performance in humans, the correlation between CAB delivered by MAPs and that delivered by IM injection (the conventional administration route) in terms of PK behavior should be investigated and then extrapolated to PK behavior in human post-administration by the same route (IM injection). This can be achieved by calculating the apparent half-life ($t_{0.5}$) of CAB and using it for comparison.

Calculating $t_{0.5}$ of CAB LA post-IM injection in rats using the PK profile produced upon injecting 10 mg/rat (equates to $\approx 40 \text{ mg/kg}$) was rather difficult, since the drug reached C_{max} and remained around that concentration until the end of the study. Therefore, lower doses of CAB LA of either 5 mg/rat (equates to 21.3 mg/kg) or 2.5 mg/rat (equates to 10.4 mg/kg) (Section S12, Supporting Information) were used to calculate $t_{0.5}$ and investigate the effect of the administered dose on $t_{0.5}$. This study showed that $t_{0.5}$ of CAB post-administration of CAB LA by IM injection was dose-dependent and was in the magnitude of 12.3 days (for dose of 5 mg/rat) and 9.0 days (for

dose of 2.5 mg/rat), respectively (Section S12, Supporting Information). This suggests that CAB follows “flip flop” pharmacokinetics,^[69] which means that drug persistence in the body central compartment (plasma exposure), and thus its apparent $t_{0.5}$, is dependent upon the absorption process, rather than the drug elimination process. Thus, the higher delivered dose and the slower the absorption rate, the longer the apparent $t_{0.5}$.^[69]

Taking into consideration that the administered CAB LA dose of 2.5 mg/rat (equates to 10.4 mg/kg) is closely related to the CAB LA dose of 800 mg ($\approx 11.4 \text{ mg/kg}$) in humans without allometric scaling,^[13] the apparent $t_{0.5}$ (≈ 9.0 days) of CAB in rats is ≈ 4.4 -fold shorter than that (≈ 40 days [25–54 days]) observed in humans post administering CAB LA by the same route. This is consistent with the fact that rats generally eliminate drugs at faster rates than humans.^[64]

The apparent $t_{0.5}$ of CAB achieved post-applying CAB LA-MAP and CAB Na-MAP were of the magnitude of ≈ 7.3 and ≈ 5.8 days, respectively. These are within the same range of that (≈ 9.0 day) achieved by CAB LA administered by IM injection and represent a duration 5.4- to 6.8-fold shorter than that (≈ 40 days) observed in humans post administering CAB LA by IM injection. This suggests it is most likely that, if either CAB LA or CAB Na were delivered by MAPs in a human, they would behave pharmacokinetically in a similar fashion to CAB LA delivered by IM injection.

The apparent $t_{0.5}$ of CAB in rats, calculated here, is of great importance, as it can be also used to estimate the dosing interval (T) in rats that mimics the currently used dosing intervals in humans (monthly or bimonthly), providing that closely related doses are used, without allometric scaling. Currently, in the monthly dosing regimen in humans, the $T/t_{0.5}$ ratio (28/40) is of the magnitude of 0.70. This suggests that a weekly (≈ 6.3 days) dosing interval in rats, (where the $T/t_{0.5}$ ratio would be $= 6.3/9 = 0.70$) would be a fair and reasonable approximation to the monthly dosing interval in humans.

Taken all together, the results demonstrated that both CAB LA-MAP and CAB Na-MAP were successfully inserted in the skin, dissolved, and deposited comparable and substantial amounts of their drug cargo ($\approx 20\%$), which were consistent with *ex vivo* results. The delivered doses by both MAPs were able to achieve drug plasma levels over 4× PA-IC₉₀ over 28 days. Thus, both MAPs have potential to be used in ID delivery of CAB and could be used interchangeably. Although CAB FA-MAP exhibited similar properties *in vivo*, its delivery efficiency was very low ($\approx 9\%$) in comparison, being $\approx 50\%$ of that achieved by the other two MAPs, diminishing its potential for use.

2.6.2. CAB Pharmacokinetics After a Weekly Repeated Dose of CAB LA-MAP

To achieve the desired therapeutic effects, it is essential to use a robust drug delivery system that delivers a consistent dose upon each application and a dosing regimen that leads to drug accumulation to achieve and maintain steady-state drug concentrations in plasma (C_{ss}) within therapeutic levels. Therefore, in this study, in addition to safety and tolerability, we aimed i) to evaluate the ability of MAPs to repeatedly deliver a consistent dose post each application (MAP robustness) and

Table 2. CAB pharmacokinetic parameters in Sprague Dawley rats following administering a repeated once-weekly dose of CAB LA by either IM or ID injection or MAP application. Data are reported as means \pm SD, $n \geq 5$.

Cohort no.	Drug form used/ admin. route/device	Dose [mg/kg]	Experimental PK parameters					Dose/body weight-normalized PK parameters ^{a)}		
			$T_{\max-1}$ [days]	$T_{\max-ss}$ [days]	$C_{\max-1}$ [$\mu\text{g mL}^{-1}$]	$C_{\max-ss}$ [$\mu\text{g mL}^{-1}$]	$C_{42 \text{ days}}$ [$\mu\text{g mL}^{-1}$]	norm- $C_{\max-1}$ [$\mu\text{g mL}^{-1}$]	norm- $C_{\max-ss}$ [$\mu\text{g mL}^{-1}$]	norm- $C_{42 \text{ days}}$ [$\mu\text{g mL}^{-1}$]
8	CAB LA/IM	11.3 (± 1.3)	7	15	54.5 (± 6.8)	111.7 (± 4.5)	33.8 (± 8.5)	48.4 (± 6.0)	100.3 (± 4.0)	29.9 (± 7.5)
9	CAB LA/ID	10.8 (± 0.4)	7	22	28.8 (± 4.4)	85.0 (± 8.4)	48.0 (± 5.8)	26.7 (± 4.1)	78.2 (± 7.7)	44.4 (± 5.4)
10	CAB LA/4-MAP	51.9 (± 1.8)	4	15	35.1 (± 4.6)	60.3 (± 10.7)	11.2 (± 2.2)	27.1 (± 3.5)	46.7 (± 8.2)	8.6 (± 1.7)
11	CAB LA/2-MAP	25.8 (± 0.9)	4	15	17.5 (± 5.5)	43.1 (± 7.9)	9.6 (± 3.2)	13.6 (± 4.2)	33.4 (± 6.2)	7.4 (± 2.5)

^{a)}The dose/body weight used for normalization was 10 mg/kg for cohorts 8 and 9; it was 40 and 20 mg/kg for cohorts 10 and 11, respectively, as described in the PK parameters calculation (Section S10, Supporting Information).

the effect of MAP-delivered dose on CAB PK and ii) to assess whether repeated dosing that approximately mimics a monthly dosing regimen in humans would lead to drug accumulation and achieve steady-state drug plasma levels within the therapeutic concentration range, that is, $4 \times \text{PA-IC}_{90}$.

Since CAB LA is the established form of the drug and the previous in vivo study (where single doses were administered) demonstrated that CAB Na-MAP and CAB LA-MAP produced comparable PK profiles, the finalized CAB LA-MAP was selected as representative here.

Taking into consideration the results of the previous in vivo study in terms of the relative bioavailability of CAB from MAPs, the apparent $t_{0.5}$ and the study aims, a dose of 2.5 mg/rat was selected as the dose to be administered to the rats once-weekly (to mimic once-monthly dosing in humans) on each of 4 weeks, in addition to other cohorts that received half of the dose by MAPs for the sake of comparison.

To this end, four cohorts were allocated for this study, two cohorts (cohorts 8 and 9) were used as controls, where each rat received a dose of 2.5 mg/rat of CAB LA (four times diluted by water) by IM or ID injection, respectively, and in the other two cohorts, each rat received the drug by MAPs either as $4 \times$ MAPs (cohort 10) or $2 \times$ MAPs (cohort 11). Plasma samples collected at predetermined time intervals over 42 days were analyzed by UPLC-MS-MS (Section S10, Supporting Information). CAB PK profiles are presented in Figure 5F and the key PK parameters, including the maximum drug concentration ($C_{\max-1}$) after the first dose, the time of maximum concentration ($T_{\max-1}$) after the first dose, the maximum drug concentration at the pseudo-steady-state ($C_{\max-ss}$), the time to reach the pseudo-steady-state maximum concentration ($T_{\max-ss}$), and the minimum drug concentration at the last sampling point (C_{trough}), that is, (C_{42}) at day 42, and the dose/body weight normalized PK parameters were determined (Section S11, Supporting Information) (Table 2) and used for comparison with the corresponding PK parameters achieved post-administering the drug by IM injection. Finally, drug accumulation ($C_{\max-ss}/C_{\max-1}$) and depreciation ($C_{\max-ss}/C_{42}$) rates for each cohort were calculated and reported.

As can be seen from Figure 5F, in all cohorts the drug appeared in plasma within 1 h (the first sampling point) post-

dosing and continued increasing in concentration upon administration of further doses. The plasma levels showed various patterns and that were dependent upon the administration route/device and the administered dose.

In those rats that received the drug by IM injection, CAB PK profiles showed a high plasma exposure, even higher than that in cohort 1 (where rats received 10 mg/rat doses), which is consistent with complete drug delivery and the effect of diluting CAB LA. The drug appeared in plasma within 1 h (the first sampling point) post-dosing and increased in concentration gradually to reach $C_{\max-1}$ at $T_{\max-1}$ (7 days). Administering further drug doses resulted in drug accumulation and continuous increase in drug plasma concentrations until day 15 ($T_{\max-ss} = 15$ days) (1-day post 3rd dose), where the drug reached its $C_{\max-ss}$ and remained around this concentration for almost two weeks until day 28. Subsequently, drug concentration declined gradually to reach its (C_{42}) at day 42. The drug concentration accumulation rate ($C_{\max-ss}/C_{\max-1}$) was ≈ 2.1 . Drug concentration depreciation rate ($C_{\max-ss}/C_{42}$) was 3.4.

In those rats that received the drug by ID injection (cohort 9), as expected, CAB exhibited a parallel PK profile. However, as in the single-dose study, $T_{\max-ss}$ was longer (22 days, 1-day post the 4th dose). Also, $C_{\max-1}$, $C_{\max-ss}$, and C_{42} were significantly ($p < 0.05$) lower than those achieved by IM injection (Table 2). The drug concentration accumulation rate and depreciation rate were of the magnitude of ≈ 2.9 and 1.8, respectively, indicating that skin can retain the drug to a greater extent than muscle tissues. This is consistent with a decreased absorption rate in the skin due to the inherited differences in the anatomy and physiology between the skin and the muscle tissues, as discussed in the previous section.

Concerning CAB PK profiles, in rats that received $4 \times$ CAB LA-MAP (cohort 10), CAB again appeared in plasma within 1 h post-dosing and increased in concentration gradually to reach its C_{\max} after the first dose ($C_{\max-1}$) at day 4 ($T_{\max-1}$). Administering further drug doses, similarly to IM injection, resulted in drug accumulation and continuous increase in drug concentrations until day 15 (T_{ss}) (1-day post 3rd dose), where the drug reached its $C_{\max-ss}$ and remained around this concentration for almost two weeks until day 28, implying that the drug

was accumulating in the skin, leading to drug concentrations fluctuating around $C_{\max-ss}$ and then declining gradually to reach C_{42} ($\approx 11.2 \mu\text{g mL}^{-1}$) at day 42. The drug concentration accumulation rate and depreciation rates were of the magnitude of ≈ 1.7 and ≈ 5.4 , respectively, which are more closely related to those observed post-IM injection, rather than post-ID injection. This was again consistent with a relatively faster absorption rate (than from ID depots), due to the relatively large surface area provided by hundreds of micro-depots deposited in the skin by MAPs.

It is worth mentioning that the produced normalized $C_{\max-1}$, $C_{\max-ss}$, and C_{42} were 56.1%, 45.3%, and 29.4%, respectively, of the corresponding PK parameters observed after IM injection. However, if we take into consideration the dilution factor (four times dilution resulted in increased C_{\max} , (Section S12, Supporting Information) effect on those parameters produced by IM injection, $C_{\max-1}$ and C_{ss} produced by applying 4×CAB LA-MAP would be expected to be higher or equal to those produced if undiluted equivalent CAB LA doss were administered by IM injection.

In cohort 11 (rats that received 2× CAB LA-MAP containing 5.86 mg CAB LA, half of the dose received by rats in cohort 10), the plasma CAB concentrations were almost halved. For example, norm- $C_{\max-1}$ after the first dose was $\approx 13.6 \mu\text{g mL}^{-1}$, which is $\approx 50.3\%$ of that observed after applying 4× CAB LA-MAP ($\approx 27.1 \mu\text{g mL}^{-1}$) (Table 2), indicating that the MAPs were robust and can repeatedly deliver a consistent dose, which is proportional to the number of MAPs applied. The $C_{\max-ss}$ ($\approx 33.4 \mu\text{g mL}^{-1}$) was $\approx 72\%$ of that observed after applying 4× CAB LA-MAP ($\approx 33.4 \mu\text{g mL}^{-1}$), which is consistent with the reduced clearance due to the reduced dose. Also, drug plasma levels gradually decreased to reach C_{42} ($\approx 7.4 \mu\text{g mL}^{-1}$) at day 42, which equates to $\approx 86.1\%$ that observed after applying 4× CAB LA-MAP. This is still 11.1-fold above 4× PA-IC₉₀. The drug concentration accumulation rate and depreciation rates were of the magnitude of ≈ 2.5 and ≈ 4.5 , respectively. These are within the same range as the previous cohort, where 4× MAPs were applied, indicating that administering two different doses that varied by a factor of 2 did not significantly affect CAB PK in rats.

This study confirms that MAP administration of long-acting CAB is robust and was able to deliver a consistent dose upon application and achieve pseudo-steady-state concentrations after the 3rd dose, similar to that achieved with IM injection. CAB concentration patterns at steady-state were similar to those observed in humans following 800 mg loading dose by IM injection with a maintenance dose of 200 mg monthly by either IM or subcutaneous injection.^[13,70]

2.6.3. CAB-MAP Safety and Tolerability

Safety and tolerability are of paramount importance for any drug delivery system. We were testing our MAPs for the first time in vivo, and we were concerned about any potential side effects that may be induced. Therefore, MAP application sites were inspected for any signs of toxicity. Rat weights and behavior in all treatment groups, including controls, were monitored over the study periods and compared with a negative

control cohort (where rats did not receive any drug). All treatments were well tolerated with no deaths or serious adverse effects observed. Importantly, rats that received the drug by MAPs did not show any sign of apparent irritation, infection, or any other skin complications post-application, apart from the expected mild erythema, which always subsided within a few hours after MAP removal. Additionally, no significant differences in weight gain were observed between the control and treatment groups (Section S4, Supporting Information), indicating that MAPs were safe and well-tolerated.

2.7. MAP Size Estimation for Human Use and Special Considerations for Application

Our studies have demonstrated that our MAP was able to deliver substantial amount of CAB LA and its less expensive micronized form, CAB Na, ID and maintaining its long-acting PK profile over 28 days in rats such that drug plasma levels were greater than 4× PA-IC₉₀. This was so, even though the CAB LA apparent half-life in rats was ≈ 4.4 -fold shorter than that reported in humans (9.0 days in rats vs 40 days in human).^[13] The once-weekly repeated doses in rats (that mimics once-monthly in humans) showed our MAP was robust and led to drug accumulation in the plasma. Plasma drug concentrations reached pseudo-steady-state at 1-day post the 3rd dose and remained around that concentration for 2 weeks, before declining gradually to reach C_{trough} that was >10 -fold higher than 4× PA-IC₉₀ at day 42. The PK pattern observed in our study resembles that produced upon applying an 800 mg loading dose flowed by repeated 200 mg maintenance doses once-monthly in humans, which achieved a consistent steady-state concentration above 4× PA-IC₉₀.^[71]

Although rats are a good model for screening long-acting formulations,^[63] the inherent differences between rats and humans, make it rather difficult, at this stage, to accurately calculate the MAP size needed to achieve similar efficacy of prevention from HIV-1 transmission. However, we can still use in vivo relative bioavailability and the estimated amount of drug delivered per unit area of MAP to make an approximate estimation of MAP size that would be required to deliver the necessary dose in humans in two dosing scenarios (monthly or weekly).

Since we are the first to develop such systems, no previous studies have specifically dealt with the pharmacokinetics of CAB LA-MAPs in humans. However, a whole-body physiologically based pharmacokinetic (PBPK) model has been recently developed for the in silico prediction of the optimal CAB LA-MAP dosing.^[72] The authors have validated the PBPK model for CAB LA pharmacokinetic prediction and employed it to estimate the required CAB LA dose that should be delivered ID by either MAP or hypodermic injection to achieve drug systemic exposure comparable to that produced by once-monthly 400 mg IM injection and maintain plasma concentrations at twice the 4× PA-IC₉₀ (i.e., $1.2 \mu\text{g mL}^{-1}$).^[72] Interestingly, the authors have reported that a loading dose of 360 mg of CAB LA, followed by 180 mg monthly or 60 mg weekly administered ID either by hypodermic injection or by MAP would produce CAB LA plasma levels comparable to those achieved by a 400 mg IM dose once monthly. Therefore, using the estimated CAB LA

doses from the PBPK model and the percentage of the dose that was delivered by MAPs (containing 3 mg/0.5 cm²) from our in vivo PK studies on rats, where the amount of drug delivered was ≈0.585 mg/0.5 cm² MAP, we cautiously estimated the patch sizes that would be required for monthly or weekly dosing in adult humans.

Using these data set, it was estimated that MAP size that would be required to deliver a loading dose of 360 mg and a monthly maintenance dose of 180 mg would be of the magnitude of ≈307 and ≈153.5 cm², respectively. Such MAP sizes are quite large and likely unrealistic for patient application. However, the MAP size to deliver 60 mg (≈50 cm²) for weekly dosing is very feasible, especially if the therapy is initiated by administering a large dose of CAB LA (e.g., 800 mg) by IM injection, similar to the currently employed dosing regimen^[10] and then followed by MAP application as a maintenance dose on a weekly basis. Indeed, this MAP size is within the range of available conventional transdermal patches, with sizes up to 140 cm² found on the market. Common patch sizes include, for example, Nicotinell (nicotine) patches measuring 30 cm² and Duragesic CII (fentanyl) patches measuring 32 and 42 cm². Accordingly, the comparable patch size for weekly maintenance dosing of CAB estimated here (≈50 cm²) is quite promising.

In considering the potential value proposition of MAP in LICs, cost-effectiveness is essential. Therefore, manual application (without an additional applicator) would be preferable if it can be demonstrated to result in the reliable application by target users and also result in a lower-cost product. To this end, a patient must be properly instructed how to apply the MAP and a feedback indicator documenting successful insertion be incorporated to increase client confidence. Our research team and others have previously published user feasibility studies, with results indicating that MAP can be reproducibly self-applied to the skin without the need for complex applicators or specialist personnel, including larger, multi-array patches.^[73] An assessment of a MAP prototype among target audiences at risk of HIV in Uganda and South Africa found that MAP technology is acceptable and that self-administration is highly valued.^[74] A discreet, painless drug delivery system such as an HIV PrEP MAP could be an important option for women and men in LICs who may have difficulty accepting or accessing other PrEP options that are currently available or in development, including pills, injections, and vaginal rings. Once trained, clients could apply an HIV PrEP MAP by themselves outside a clinic setting. MAP-based drug delivery has the potential not only to improve access, acceptability, and adherence for HIV PrEP but also could be used to deliver other drug molecules.

Our in vivo studies showed that CAB-MAPs were safe and well-tolerated in rats and did not cause irritation or infection, but only mild erythema, which subsided within a few hours post MAP removal. However, to facilitate MAP translation to human application, patient acceptability and safety of MAPs should be investigated further.

2.8. Limitation and Future Outlook

Although our novel MAPs have demonstrated promising properties and capabilities, they have some limitations—the first

of these lies in delivery efficiency. MAPs were able to deliver substantial amounts of the loaded dose. Nevertheless, the delivery efficiency was suboptimal (≈13–17% ex vivo and ≈20% in vivo). The second limitation was in the in vivo experimental conditions. Even though 60 min was sufficient for the MAP tips to completely dissolve in the skin (ex vivo), MAPs had to be applied for 24 h, as their removal required using anesthesia, which is only permitted once per 24 h (as per our Institutional Animal License). This precluded us from evaluating the actual wear time in vivo to benefit from fabricating bilayer MAPs with fast-dissolving tips and slowly dissolving baseplates. Future studies must be carried out to further optimize CAB delivery efficiency by improving MAP design to increase needle insertion capability and concentrating the drug in the MAP tip ends to avoid wastage of the drug. The MAP design can potentially be improved by employing various strategies, such as increasing the aspect ratio, increasing the density of the needles per MAP, increasing the interspacing, or trying different needle shapes. Further studies will also be needed to evaluate the dissolution kinetics and drug deposition at various time points in vivo. We are currently working to resolve these issues.

3. Conclusion

These prototype MAPs represent a minimally invasive drug delivery system, which can potentially be self-administered for long-acting delivery of clinically relevant doses of CAB for HIV prevention. This work with tip-localized drug loading resulted in a considerable increase in loading capacity in a relatively small MAP compared with many other MAP types. This could mean that microneedle technologies will be increasingly considered for the delivery of a much wider range of drugs. Further studies are now required, first to enhance delivery efficiency and then to evaluate pharmacokinetics and safety in humans, before these highly promising MAPs can be taken forward for more extensive clinical evaluation in HIV prevention.

4. Experimental Section

Materials: CAB LA vials for IM injection with drug content (400 mg/2 mL), and micronized powders of CAB Na and CAB FA, were kindly supplied by ViiV Healthcare (North Carolina, USA). Poly(vinyl alcohol) of molecular weight (MW) 9–10 kDa, 80% hydrolyzed (PVA 10K) and of MW 31–50 kDa, 87–89% hydrolyzed (PVA 50K) were purchased from Sigma-Aldrich (Dorset, UK). Poly(vinyl pyrrolidone) K29-32 of MW 58 kDa (PVP) was a gift from Ashland (Kidderminster, UK). Pullulan (viscosity: 133 mm² s⁻¹, 10%w/w, Ubbelohde type viscometer, average MW 200 kDa) was kindly provided by Hayashibara Co. Ltd. (Tokyo, Japan). Hyaluronic acid (HA) (Hyabest (S) LF-P, sodium hyaluronate 99.9% purity, MW 250–400 kDa range) was obtained from Kewpie Corporation Fine Chemical Division (Tokyo, Japan). Liquid silicone rubber (DDR-4320) was purchased from Nusil Technology (Buckinghamshire, UK). Ultrapure water was obtained from a water purification system (Elga PURELAB DV 25, Veolia Water Systems, Dublin, Ireland). All other chemicals and materials were of analytical reagent grade supplied by Sigma-Aldrich (Dorset, UK).

Development and Fabrication of MAP Design: Briefly, CAD was used to create the novel MAP design (Figure 2A), which was used to produce a master template (Figure 2B,C) by 2-photon polymerization of IP-S resins (acrylate-based polymers) using a photonic professional GT 3D

printer system (Nanoscribe GmbH, Germany).^[31,75] Subsequently, the master template was attached to a PLA-based holder (Figure 2C) and then used to prepare MAP female molds using the transparent LSR9-9508-30 silicone elastomer mix (Figure 2D). The silicone-filled template was then centrifuged at 3500 rpm for 15 min to remove any residual air bubbles and cured for 3–6 h at 60 °C. The master template was allowed to cool down before the removal of the PDMS mold. The PDMS mold (Figure 2E) was then used to manufacture the bilayer CAB-MAPs.

Fabrication of Bilayer CAB-MAPs: Bilayer CAB LA-MAPs were prepared using the finalized CAB LA-loaded polymeric blend (Section S1, Supporting Information) to form the first MAP layer and the optimized polymeric blend (Section S2, Supporting Information) for the second MAP layer by a two-step casting approach using the same positive pressure chamber as depicted in Figure 2F. Briefly, 100 mg of the finalized CAB LA-loaded hydrogel was dispensed onto the PDMS mold of the developed MAP and then placed in the positive pressure chamber at 5 bars for 3 min. After that, the PDMS molds were removed from the chamber. The excess of the drug-loaded hydrogel was carefully scraped using a stainless-steel spatula, and the molds were immediately placed again in the chamber with 5 bars of pressure for 15 min. Subsequently, the PDMS molds were removed from the chamber, and the first MAP layer was dried overnight at room temperature. The second MAP layer was then prepared by pouring the optimized drug-free polymeric blend on top of the first layer under vacuum and placing the molds in a positive pressure chamber at 5 bars for 15 min. Finally, the bilayer CAB LA-MAP was dried at room temperature for 24 h, and then at 37 °C for 24 h before being gently removed from the molds and stored in a desiccator until further testing or use.

Bilayer micronized CAB-MAPs were prepared using either the finalized CAB Na-loaded hydrogel or finalized CAB FA-loaded hydrogel to form the first MAP layer (Section S4, Supporting Information) and the optimized drug-free hydrogel for the second MAP layer by a two-step casting approach following the same fabrication procedures as described above.

Determination of CAB-MAP Drug Content: MAP drug content was determined by two methods: directly by dissolving the MAP and then analyzing its drug content; or indirectly by calculating the theoretical drug loading per MAP tips based on its dimensions, the needle-free patch density, and drug content.

To determine CAB content in the three different forms of bilayer CAB-MAP in addition to a CAB LA-loaded needle-free patch, a direct method was employed. In triplicate, a sample of the designated MAP/patch was first dissolved in 5 mL of DI water. Following its complete dissolution, 100 μ L of the resultant suspension was transferred to 1.5 mL tubes and mixed vigorously with 0.9 mL acetonitrile. This process allowed the drug to be completely dissolved and led to precipitation of water-soluble polymers. The resultant suspension was subsequently centrifuged at 14800 rpm for 15 min, and 100 μ L of the clear supernatant solution was collected and analyzed after making an appropriate dilution with acetonitrile by the validated HPLC method.

Assessment of CAB-MAP Mechanical and Insertion Properties: A TA.XT2 texture analyzer (Stable Micro Systems, Haslemere, UK) in compression mode was used to determine mechanical and insertion properties of the fabricated MAPs, namely monolayer CAB LA-MAP, drug free-MAP, and the finalized bilayer CAB LA-MAP, CAB Na-MAP, and CAB FA-MAP, as previously described.^[51,76,77] Briefly, the MAP was attached to a cylindrical probe (cross-sectional area 1.5 cm²), the texture analyzer arm moved vertically downward at a speed of 0.5 mm s⁻¹, and the MAP was compressed against a flat aluminum block (Figure 4B). A force of 32 N was applied for 30 s before the probe moved upward again. The length of individual needles in each MAP was measured before and after compression using a Leica EZ4W stereo microscope (Leica Microsystems, Milton Keynes, UK). The percentage reduction of microneedle heights was calculated and reported.

To evaluate MAP insertion properties, which are solely dependent on the mechanical property and geometry of the MAP, the finalized bilayer CAB LA-MAP was selected as an exemplar, and its insertion properties into a skin-simulant membrane (Parafilm M) were first assessed

employing the same experimental setup (speed 0.5 mm s⁻¹, force 32 N) as in the mechanical properties assessment. However, the tested MAP was moved downward to be compressed against a stack of 8 layers of Parafilm M (Bemis Inc., Soignies, Belgium) as previously described.^[78] Then, the insertion depth of the MAP needles was determined indirectly by measuring the distance between MAP baseplate and the first layer of the Parafilm M using OCT (EX1301 OCT Microscope Michelson Diagnostics Ltd., Kent, UK) and the imaging software ImageJ (National Institutes of Health, Bethesda, MD, USA). The indirect measurement of MAP needle insertion depth was done due to opaqueness of the drug-loaded tips, which prevent their accurate visualization by the OCT microscope.

To increase our confidence in the ability of the finalized CAB LA-MAP to be inserted into the skin, their insertion into two skin models was also evaluated. These included an excised full-thickness neonatal porcine skin, which is a good model for human skin,^[51,55,58,79] and full-thickness rat skin. The same experimental setup for MAP insertion into the Parafilm M was again used. To achieve this, skin samples were obtained from stillborn piglets or Sprague Dawley rats. After birth, they were stored immediately at –20 °C and thawed for two days before being skinned. Full-thickness skin was cut into pieces and stored at –20 °C until further use. To do the insertion test, skin samples were immersed in PBS 10 mM (pH 7.4) for 30 min for thawing and hydration and then shaved before use. After that, the skin samples were cleaned and then left in PBS solution for another 30 min at 32 \pm 1 °C for equilibration, before being blotted dry using a tissue paper and used for testing. The MAP needle insertion into the skin was monitored again using the OCT microscope as previously described.

SEM Studies: SEM was used to examine the drug particulate morphology and distribution within the first CAB-MAP layer matrix. To achieve this, samples from the three different forms of bilayer CAB-MAP (namely, CAB LA-MAP, CAB Na-MAP, and CAB FA-MAP) were affixed onto a sticky carbon tape, sputter-coated at 2.5 kV, 18 mA with gold for 45 s (POLARON E5150, Gold Sputter Coater, Quorum Technologies, East Sussex, UK) and viewed under SEM using a Quanta FEG 250 benchtop SEM (FEI, Hillsboro, OR, USA) at an acceleration voltage of 10–20 kV under high chamber pressure (8×10^{-5} mbar).

XRD Measurements: The X-ray measurements were carried out using a benchtop XRD (Miniflex, Rigaku, Neu-Isenburg, Germany) equipped with Ni-filtered, Cu K β radiation, at a voltage of 30 kV and a current of 15 mA. The drug-loaded tips of CAB LA-MAP, CAB Na-MAP, and CAB FA-MAP were cut using a scalpel and then pulverized using stainless-steel beads and a high-speed sample homogenizer for 60 s. Then pulverized CAB-MAP and their pure related drugs were packed individually into the rotating sample holder and analyzed. The obtained data were typically collected by scanning at a range of 3°–60° in a continuous mode with a scanning rate of 2° min⁻¹.

DSC Studies: Drug-polymer interaction in the CAB-MAP was evaluated using a DSC (NETZSCH DSC 200 F3 Maia (NETZSCH, Geratebau GmbH, Selb/Germany)). Again, the drug-loaded tips of CAB LA-MAP, CAB Na-MAP, and CAB FA-MAP were cut using a scalpel and then pulverized using stainless-steel beads and a high-speed sample homogenizer (TissueLyser LT, Qiagen Corp, Manchester, UK) for 60 s. Then pulverized CAB-MAP and their pure related drugs were assayed thermally. The sample were assessed thermally in a range from 10 to 200 °C at 10 °C min⁻¹ and the gas flow rate was 50 mL min⁻¹.

Measurement of CAB LA Particle Size: To further evaluate the effects of MAP polymers and fabrication process on CAB LA particle size and PDI, CAB LA-MAP were dissolved in 10 mL of DI water. After appropriate dilution, the characteristics of CAB LA, namely particle size and PDI were determined using a NanoBrook Omni particle sizer as described in the previous section. The results obtained were compared to the initial characteristics of the CAB LA.

Evaluation of MAP Dissolution Kinetics in the Skin (Ex Vivo) and Drug Deposition: These studies were performed using full-thickness neonatal porcine as described previously.^[37] Briefly, the skin samples were prepared as described in the previous section and then the skin samples were placed on paper tissue sheets soaked with 10 mM PBS (pH 7.4) solution to maintain skin hydration and placed in a weighing boat. To

mimic the human skin temperature, the skin samples were placed in a preheated incubator for 30 min at 32 ± 1 °C. As illustrated in Figure 4H, the selected MAPs were subsequently inserted into the skin manually using thumb pressure for 30 s. After that, a 13 g cylindrical stainless-steel block was placed on top of each MAP to keep it in place, and then the skin samples were incubated again in the incubator at 32 ± 1 °C. To prevent skin drying, another weighing boat was placed on the top and 10 mm PBS (pH 7.4) solution was added to maintain skin hydration. The inserted MAPs were then removed from the skin at predetermined time intervals. For MAPs that were used to develop and optimize the first and the second MAP layer, namely monolayer CAB LA-MAP and drug free-MAP, these were applied only for 30 min. However, for the finalized bilayer CAB-MAPs, namely CAB LA-MAP, CAB Na-MAP, and CAB FA-MAP, these were applied for 5, 15, 25, and 60 min and 24 h. MAP shaft height was measured before and after insertion using the light microscope, and the percentage MAP needles height reduction was determined and reported (Figure 4I).

To evaluate drug deposition in the skin (ex vivo) from the finalized bilayer CAB-MAPs, following applications, MAPs remaining on the skin surface were carefully removed and then the skin surface was thoroughly cleaned by applying 3×1 mL of PBS (pH 7.4) solution and gently wiped with a wet paper tissue. The skin at the MAP application site was then visualized using a Leica EZ4W stereo microscope and then harvested using a biopsy punch (5.0 mm diameter) (Stiefel, Middlesex, UK) and stored in Eppendorf tubes at -20 °C until further processing and analysis using a validated HPLC-UV method described in the pharmaceutical analysis section.

In Vivo Studies: The in vivo studies were conducted according to the policy of the Federation of European Laboratory Animal Science Associations and the European Convention for the protection of vertebrate animals used for experimental and other scientific purposes, with the implementation of the principles of the 3Rs (replacement, reduction, and refinement). These studies were performed under project license no. 2794 and personal licenses nos. 1747 and 1892 at the Biological Services Unit, Queens University Belfast (UK) after obtaining the required ethical permission from the Queen's University Animal Welfare and Ethics Review Board.

These studies aimed to evaluate in vivo safety and performance of the finalized bilayer CAB-MAPs (namely CAB LA-MAP, CAB Na-MAP, and CAB FA-MAP) post applying a single dose and multiple doses in comparison with three controls using Sprague Dawley rats as a good preclinical model for screening and evaluating the pharmacokinetics of long-acting drugs.^[63] The experimental design and procedures details are provided in (Section S8, Supporting Information).

Pharmaceutical Analysis: Samples collected from the in vitro, ex vivo, and in vivo studies where drug content measuring was required were first processed as per matrix and then analyzed employing an appropriate analytical method as detailed in (Section S10, Supporting Information).

Statistical Analysis: All results were expressed as means \pm standard deviation (SD), $n \geq 3$. These were calculated using Microsoft Excel 2013 (Microsoft Corporation, Redmond, USA). Statistical analysis was carried out using GraphPad Prism version 6 (GraphPad Software, San Diego, California, USA) followed by Tukey's multiple comparisons post-hoc test and *t*-test for two-group comparisons. A value of $p < 0.05$ was considered statistically significant.

Supporting Information

Supporting Information is available from the Wiley Online Library or from the author.

Acknowledgements

I.A.T. and L.K.V. contributed equally to the work. Thanks to Viiv Healthcare for supplying CAB LA injectable formulation, the micronized

cabotegravir sodium and cabotegravir free acid. Thanks to Stephen Lloyd from the Biological Services Unit at Queen's University Belfast for his help while performing the in vivo studies. The authors would also like to thank the PATH team members who contributed to the strategic direction of this work and/or provided review and copyediting support, including Abra Greene, Maggie Kilbourne-Brook, Annie Rein-Weston, Jill Sherman-Konkle, and Darin Zehrung. This project was made possible by the generous support of the American people through the United States Agency for International Development (USAID) through the United States President's Emergency Plan for AIDS Relief (PEPFAR), under the terms of Cooperative Agreement #AID-OAA-A-17-00015. The contents are the responsibility of QUB and PATH and do not necessarily reflect the views of USAID, PEPFAR, or the United States government. Also, this work was supported in part by EPSRC grant EP/S028919/1 and Wellcome Trust grant WT094085MA.

Conflict of Interest

R.F.D. is an inventor of patents that have been licensed to companies developing microneedle-based products and is a paid advisor to companies developing microneedle-based products. The resulting potential conflict of interest has been disclosed and is managed by Queen's University Belfast. The companies had no role in the design of the manuscript, in the collection, analyses, or interpretation of the various studies reviewed, in the writing of the manuscript or in the decision to publish.

Data Availability Statement

Research data are not shared.

Keywords

cabotegravir, dissolving microarray patch, HIV, long-acting drugs, pre-exposure prophylaxis

Received: July 20, 2021

Revised: September 15, 2021

Published online:

- [1] T. R. Kemnic, P. G. Gulick, *HIV Antiretroviral Therapy*, StatPearls Publishing, Treasure Island, FL 2019.
- [2] World Health Organization, <https://www.who.int/data/gho/data/themes/hiv-aids> (accessed: March 2021).
- [3] T. Girum, A. Wasie, A. Worku, *BMC Infect. Dis.* 2018, 18, 320.
- [4] J.-M. Molina, I. Charreau, B. Spire, L. Cotte, J. Chas, C. Capitant, C. Tremblay, D. Rojas-Castro, E. Cua, A. Pasquet, C. Bernaud, C. Pintado, C. Delaugerre, L. Sagaon-Teyssier, S. Le Mestre, C. Chidiac, G. Pialoux, D. Ponscarne, J. Fonsart, D. Thompson, M. A. Wainberg, V. Doré, L. Meyer, *Lancet HIV* 2017, 4, e402.
- [5] E. J. Arts, D. J. Hazuda, *Cold Spring Harbor Perspect. Med.* 2012, 2, a007161.
- [6] Y. S. Marfatia, S. K. Jose, R. R. Baxi, R. J. Shah, *Indian J. Sex. Transm. Dis.* 2017, 38, 1.
- [7] V. Cambiano, A. Miners, D. Dunn, S. McCormack, K. J. Ong, O. N. Gill, A. Nardone, M. Desai, N. Field, G. Hart, V. Delpech, G. Cairns, A. Rodger, A. N. Phillips, *Lancet Infect. Dis.* 2018, 18, 85.
- [8] UNAIDS, <https://www.unaids.org/en/topic/data> (accessed: March 2021).
- [9] N. Tandon, J. Mao, A. Shprecher, A. J. Anderson, F. Cao, X. Jiao, K. Brown, *Curr. Med. Res. Opin.* 2019, 35, 63.

- [10] R. J. Landovitz, S. Li, B. Grinsztejn, H. Dawood, A. Y. Liu, M. Magnus, M. C. Hosseini-pour, R. Panchia, L. Cottle, G. Chau, P. Richardson, M. A. Marzinke, C. W. Hendrix, S. H. Eshleman, Y. Zhang, E. Tolley, J. Sugarman, R. Kofron, A. Adeyeye, D. Burns, A. R. Rinehart, D. Margolis, W. R. Spreen, M. S. Cohen, M. McCauley, J. J. Eron, *PLoS Med.* **2018**, *15*, e1002690.
- [11] D. Cattaneo, C. Gervasoni, *Eur. J. Drug Metab. Pharmacokinet.* **2019**, *44*, 319.
- [12] T. Whitfield, A. Torkington, C. van Halsema, *HIV/AIDS* **2016**, *8*, 157.
- [13] C. Trezza, S. L. Ford, W. Spreen, R. Pan, S. Piscitelli, *Curr. Opin. HIV AIDS* **2015**, *10*, 239.
- [14] US FDA, <https://www.fda.gov/drugs/human-immunodeficiency-virus-hiv/fda-approves-cabenuva-and-vocabria-treatment-hiv-1-infection> (accessed: February 2021).
- [15] ClinicalTrials.gov, <https://clinicaltrials.gov/ct2/show/NCT03299049> (accessed: January 2021).
- [16] ViiV Healthcare, <https://viivhealthcare.com/en-gb/media/press-releases/2020/november/viiv-Healthcare-announces-investigational-injectable-cabotegravir-is-superior-to-oral-standard-of-care-for-HIV-prevention-in-women/> (accessed: January 2021).
- [17] M. Markowitz, I. Frank, R. M. Grant, K. H. Mayer, R. Elion, D. Goldstein, C. Fisher, M. E. Sobieszczyk, J. E. Gallant, H. Van Tieu, W. Weinberg, D. A. Margolis, K. J. Hudson, B. S. Stancil, S. L. Ford, P. Patel, E. Gould, A. R. Rinehart, K. Y. Smith, W. R. Spreen, *Lancet HIV* **2017**, *4*, e331.
- [18] A. Isara, K. Oguzie, O. Okpogoro, *Ann. Med. Health Sci. Res.* **2015**, *5*, 392.
- [19] A. O. Olaleye, O. A. Ogundele, B. I. Awokola, O. S. Olatunya, O. A. Olaleye, T. Adeyanju, A. G. Omisore, *Int. J. Occup. Saf. Health* **2013**, *3*, 1.
- [20] V. Goel, D. Kumar, R. Lingaiah, S. Singh, *J. Lab. Physicians* **2017**, *9*, 020.
- [21] L. K. Vora, K. Moffatt, I. A. Tekko, A. J. Paredes, F. Volpe-Zanutto, D. Mishra, K. Peng, R. R. Singh Thakur, R. F. Donnelly, *Eur. J. Pharm. Biopharm.* **2021**, *159*, 44.
- [22] E. Larrañeta, R. E. M. Lutton, A. D. Woolfson, R. F. Donnelly, *Mater. Sci. Eng., R* **2016**, *104*, 1.
- [23] M. Ventre, V. Coppola, M. Iannone, P. A. Netti, I. Tekko, E. Larrañeta, A. M. Rodgers, C. J. Scott, A. Kissenpennig, R. F. Donnelly, S. Maher, D. Losic, A. George, A. Ramachandran, in *Nanotechnologies in Preventive and Regenerative Medicine* (Eds: V. Uskoković, D. P. Uskoković), Elsevier, New York **2018**, p. 93.
- [24] A. J. Paredes, I. K. Ramöller, P. E. McKenna, M. T. A. Abbate, F. Volpe-Zanutto, L. K. Vora, M. Kilbourne-Brook, C. Jarrahian, K. Moffatt, C. Zhang, I. A. Tekko, R. F. Donnelly, *Adv. Drug Delivery Rev.* **2021**, *173*, 331.
- [25] E. McAlister, M. Kirkby, J. Domínguez-Robles, A. J. Paredes, Q. K. Anjani, K. Moffatt, L. K. Vora, A. R. J. Hutton, P. E. McKenna, E. Larrañeta, R. F. Donnelly, *Adv. Drug Delivery Rev.* **2021**, *175*, 113825.
- [26] A. J. Paredes, P. E. McKenna, I. K. Ramöller, Y. A. Naser, F. Volpe-zanutto, M. Li, M. T. A. Abbate, L. Zhao, C. Zhang, J. M. Abu-ershaid, X. Dai, R. F. Donnelly, *Adv. Funct. Mater.* **2020**, *31*, 2005792.
- [27] I. Tekko, L. Vora, M. McCrudden, C. Jarrahian, A. Rein-Weston, D. Zehring, P. Giffen, H. McCarthy, R. Donnelly, in *Controlled Release Society Annual Meeting & Exposition, CRS, Valencia* **2019**.
- [28] L. Y. Chu, S. O. Choi, M. R. Prausnitz, *J. Pharm. Sci.* **2010**, *99*, 4228.
- [29] M. Wang, L. Hu, C. Xu, *Lab Chip* **2017**, *17*, 1373.
- [30] S. D. Gittard, B. Chen, H. Xu, A. Ovsianikov, B. N. Chichkov, N. A. Monteiro-Riviere, R. J. Narayan, *J. Adhes. Sci. Technol.* **2013**, *27*, 227.
- [31] A. S. Cordeiro, I. A. Tekko, M. H. Jomaa, L. Vora, E. McAlister, F. Volpe-Zanutto, M. Nethery, P. T. Baine, N. Mitchell, D. W. McNeill, R. F. Donnelly, *Pharm. Res.* **2020**, *37*, 174.
- [32] M. T. C. McCrudden, E. Larrañeta, A. Clark, C. Jarrahian, A. Rein-Weston, B. Creelman, Y. Moyo, S. Lachau-Durand, N. Niemeijer, P. Williams, H. O. McCarthy, D. Zehring, R. F. Donnelly, *Adv. Healthcare Mater.* **2019**, *8*, 1801510.
- [33] K. Ita, *Pharmaceutics* **2015**, *7*, 90.
- [34] H. Chang, M. Zhong, S. W. T. Chew, C. Xu, *Adv. Mater. Technol.* **2020**, *5*, 1900552.
- [35] I. A. Tekko, G. Chen, J. Domínguez-Robles, R. R. S. Thakur, I. M. N. Hamdan, L. Vora, E. Larrañeta, J. C. McElnay, H. O. McCarthy, M. Rooney, R. F. Donnelly, *Int. J. Pharm.* **2020**, *586*, 119580.
- [36] A. D. Permana, I. A. Tekko, M. T. C. McCrudden, Q. K. Anjani, D. Ramadon, H. O. McCarthy, R. F. Donnelly, *J. Controlled Release* **2019**, *316*, 34.
- [37] I. A. Tekko, A. D. Permana, L. Vora, T. Hatahet, H. O. McCarthy, R. F. Donnelly, *Eur. J. Pharm. Sci.* **2020**, *152*, 105469.
- [38] M. Teodorescu, M. Bercea, S. Morariu, *Biotechnol. Adv.* **2019**, *37*, 109.
- [39] M. M. M. L. Mansour, T. B. Mahmoud, *Iran. Polym. J.* **2005**, *14*, 1022.
- [40] M. I. Baker, S. P. Walsh, Z. Schwartz, B. D. Boyan, *J. Biomed. Mater. Res., Part B* **2012**, *100B*, 1451.
- [41] T. Kamarul, G. Krishnamurthy, N. D. Salih, N. S. Ibrahim, H. R. B. Raghavendran, A. R. Suhaeb, D. S. K. Choon, *Sci. World J.* **2014**, *2014*, 905103.
- [42] I. A. Tekko, A. D. Permana, L. Vora, T. Hatahet, H. O. McCarthy, R. F. Donnelly, *Eur. J. Pharm. Sci.* **2020**, *152*, 105469.
- [43] L. B. Jenkins, F. E. Kredel, W. M. McCord, *Arch. Surg.* **1956**, *72*, 612.
- [44] W. Hespe, A. M. Meier, Y. J. Blankwater, *Arzneimittelforschung* **1977**, *27*, 1158.
- [45] T. Yamaoka, Y. Tabata, Y. Ikada, *J. Pharm. Pharmacol.* **1995**, *47*, 479.
- [46] E. M. Migdadi, A. J. Courtenay, I. A. Tekko, M. T. C. McCrudden, M. C. Kearney, E. McAlister, H. O. McCarthy, R. F. Donnelly, *J. Controlled Release* **2018**, *285*, 142.
- [47] R. E. M. Lutton, E. Larrañeta, M. C. Kearney, P. Boyd, A. D. Woolfson, R. F. Donnelly, *Int. J. Pharm.* **2015**, *494*, 417.
- [48] M. T. C. Mc Crudden, E. Larrañeta, A. Clark, C. Jarrahian, A. Rein-Weston, S. Lachau-Durand, N. Niemeijer, P. Williams, C. Haack, H. O. McCarthy, D. Zehring, R. F. Donnelly, *J. Controlled Release* **2018**, *292*, 119.
- [49] M. T. C. Mc Crudden, E. Larrañeta, A. Clark, C. Jarrahian, A. Rein-Weston, B. Creelman, Y. Moyo, S. Lachau-Durand, N. Niemeijer, P. Williams, H. O. McCarthy, D. Zehring, R. F. Donnelly, **2019**, *8*, 1801510.
- [50] S. Abdelghany, I. A. Tekko, L. Vora, E. Larrañeta, A. D. Permana, R. F. Donnelly, *Pharmaceutics* **2019**, *11*, 308.
- [51] E. Larrañeta, J. Moore, E. M. Vicente-Pérez, P. González-Vázquez, R. Lutton, A. D. Woolfson, R. F. Donnelly, *Int. J. Pharm.* **2014**, *472*, 65.
- [52] E. Larrañeta, R. E. M. Lutton, A. D. Woolfson, R. F. Donnelly, *Mater. Sci. Eng., R* **2016**, *104*, 1.
- [53] E. Larrañeta, J. Moore, E. M. Vicente-Pérez, P. González-Vázquez, R. Lutton, A. D. Woolfson, R. F. Donnelly, *Int. J. Pharm.* **2014**, *472*, 65.
- [54] R. R. S. Thakur, I. A. Tekko, F. Al-Shammari, A. A. Ali, H. McCarthy, R. F. Donnelly, *Drug Delivery Transl. Res.* **2016**, *6*, 800.
- [55] W. Meyer, *Hautarzt* **1996**, *47*, 178.
- [56] K. Peng, L. K. Vora, J. Domínguez-Robles, Y. A. Naser, M. Li, E. Larrañeta, R. F. Donnelly, *Mater. Sci. Eng., C* **2021**, *127*, 112226.
- [57] W. Li, R. N. Terry, J. Tang, M. R. Feng, S. P. Schwendeman, M. R. Prausnitz, *Nat. Biomed. Eng.* **2019**, *3*, 220.
- [58] E. Abd, S. A. Yousef, M. N. Pastore, K. Telaprolu, Y. H. Mohammed, S. Namjoshi, J. E. Grice, M. S. Roberts, *Clin. Pharmacol.: Adv. Appl.* **2016**, *8*, 163.
- [59] M. T. C. Mc Crudden, E. Larrañeta, A. Clark, C. Jarrahian, A. Rein-Weston, S. Lachau-Durand, N. Niemeijer, P. Williams, C. Haack, H. O. McCarthy, D. Zehring, R. F. Donnelly, *J. Controlled Release* **2018**, *28*, 119.

- [60] L. K. Vora, R. F. Donnelly, E. Larrañeta, P. González-Vázquez, R. R. S. Thakur, P. R. Vavia, *J. Controlled Release* **2017**, 265, 93.
- [61] A. D. Permana, M. T. C. McCrudden, R. F. Donnelly, *Pharmaceutics* **2019**, 11, 346.
- [62] ICH Topic Q 1 A (R2) Stability Testing of New Drug Substances and Products Step 5 NOTE FOR GUIDANCE ON STABILITY TESTING: STABILITY TESTING OF NEW DRUG SUBSTANCES AND PRODUCTS, **2003**.
- [63] H. Patel, P. Patel, N. Modi, P. Patel, Y. Wagh, A. George, N. Desai, N. R. Srinivas, *Xenobiotica* **2019**, 49, 415.
- [64] A. Nair, S. Jacob, *J. Basic Clin. Pharm.* **2016**, 7, 27.
- [65] C. Trezza, S. L. Ford, W. Spreen, R. Pan, S. Piscitelli, *Curr. Opin. HIV AIDS* **2015**, 10, 239.
- [66] B. M. Jucker, H. Alsaïd, M. Rambo, S. C. Lenhard, B. Hoang, F. Xie, M. R. Groseclose, S. Castellino, V. Damian, G. Bowers, M. Gupta, *J. Controlled Release* **2017**, 268, 102.
- [67] M. D. Delp, M. V. Evans, A. C. Duan, *J. Appl. Physiol.* **1998**, 85, 5.
- [68] S. M. Dizaj, Z. Vazifehasl, S. Salatin, K. Adibkia, Y. Javazadeh, *Res. Pharm. Sci.* **2015**, 10, 95.
- [69] J. A. Yáñez, C. M. Remsberg, C. L. Sayre, M. L. Forrest, N. M. Davies, *Ther. Delivery* **2011**, 2, 643.
- [70] W. Spreen, S. L. Ford, S. Chen, D. Wilfret, D. Margolis, E. Gould, S. Piscitelli, *JAIDS, J. Acquired Immune Defic. Syndr.* **2014**, 67, 481.
- [71] W. Spreen, P. Williams, D. Margolis, S. L. Ford, H. Crauwels, Y. Lou, E. Gould, M. Stevens, S. Piscitelli, *JAIDS, J. Acquired Immune Defic. Syndr.* **2014**, 67, 487.
- [72] R. K. R. Rajoli, D. J. Back, S. Rannard, C. F. Meyers, C. Flexner, A. Owen, M. Siccardi, *Clin. Pharmacokinet.* **2018**, 57, 255.
- [73] A. Ripolin, J. Quinn, E. Larrañeta, E. M. Vicente-Perez, J. Barry, R. F. Donnelly, *Int. J. Pharm.* **2017**, 521, 92.
- [74] M. K. Brook, A. Ismail, S. Magni, T. Fellows, A. R. Katahoire, F. Ayebare, *J. Int. AIDS Soc.* **2021**, 24, 10.
- [75] L. Vora, I. Tekko, M. H. Joraa, P. Baine, R. Donnelly, in *Controlled Release Society Annual Meeting & Exposition*, CRS, Valencia **2019**.
- [76] L. K. Vora, P. R. Vavia, E. Larrañeta, S. E. J. Bell, R. F. Donnelly, *J. Interdiscip. Nanomed.* **2018**, 3, 89.
- [77] I. K. Ramöller, I. A. Tekko, H. O. McCarthy, R. F. Donnelly, *Int. J. Pharm.* **2019**, 566, 299.
- [78] A. J. Paredes, F. Volpe-Zanutto, A. D. Permana, A. J. Murphy, C. J. Picco, L. K. Vora, J. A. Coulter, R. F. Donnelly, *Int. J. Pharm.* **2021**, 606, 120885.
- [79] A. Summerfield, F. Meurens, M. E. Ricklin, *Mol. Immunol.* **2015**, 66, 14.